Involvement of urinary bladder Connexin43 and the circadian clock in coordination of diurnal micturition rhythm

Hiromitsu Negoro,[1,2] Akihiro Kanematsu,[1,3] Masao Doi,[4] Sylvia O. Suadicani,[5,6] Masahiro Matsuo,[4] Masaaki Imamura,[1] Takeshi Okinami,[1] Nobuyuki Nishikawa,[1] Tomonori Oura,[7] Shigeyuki Matsui,[8] Kazuyuki Seo,[4] Motomi Tainaka,[4] Shoichi Urabe,[4] Emi Kiyokage,[9] Takeshi Todo,[10] Hitoshi Okamura,[4]* Yasuhiko Tabata,[2] and Osamu Ogawa[1]*

[1]Department of Urology, Graduate School of Medicine, Kyoto University, Sakyo, Kyoto, 606-8507, Japan;

[2]Department of Biomaterials, Institute for Frontier Medical Sciences, Sakyo, Kyoto University, Kyoto, 606-8507, Japan;

[3]Department of Urology, Hyogo College of Medicine, Nishinomiya, Hyogo, 663-8501, Japan;

[4]Department of Systems Biology, Graduate School of Pharmaceutical Sciences, Kyoto University, Sakyo, Kyoto, 606-8501, Japan;

[5]Department of Urology and [6]Dominick P. Purpura Department of Neuroscience, Albert Einstein College of Medicine, Bronx, NY, 10461, USA;

[7]Department of Biostatistics, Kyoto University School of Public Health, Sakyo, Kyoto, 606-8501, Japan;

[8]Department of Data Science, The Institute of Statistical Mathematics, Tachikawa, Tokyo, 190-0014, Japan;

[9]Department of Anatomy, Kawasaki Medical School, Kurashiki, Okayama, 701-0192, Japan;

[10]Department of Radiation Biology and Medical Genetics, Graduate School of Medicine, Osaka University, Suita, Osaka, 565-0871, Japan

Key words: connexin43, Rev-erbα, Sp1, circadian, bladder, micturition

Running Head: Bladder Cx43 and clock in circadian micturition rhythm

*Correspondence should be addressed to H.O. (okamurah@pharm.kyoto-u.ac.jp) or O.O. (ogawao@kuhp.kyoto-u.ac.jp).

Summary

Nocturnal enuresis in children and nocturia in the elderly are two highly prevalent clinical conditions, characterized by a mismatch between urine production rate in the kidneys and storage in the urinary bladder during the sleep phase. Using a novel method for automatic recording of mouse micturition, we demonstrate that connexin43 (Cx43), a bladder gap junction protein, is a negative regulator of functional bladder capacity. Bladder *Cx43* levels and functional capacity show circadian oscillations in wild-type mice, but such rhythms are completely lost in *Cry*-null mice having a dysfunctional biological clock. Bladder muscle cells have an internal clock, and show oscillations of Cx43 and gap junction function. A clock regulator, Rev-erbα, upregulates *Cx43* transcription as a co-factor of Sp1 using Sp1 *cis*-elements of the promoter. Therefore, circadian oscillation of *Cx43* is associated with the biological clock and contributes to diurnal changes in bladder capacity, which avoids disturbance of sleep by micturition.

Nocturnal enuresis is the involuntary loss of urine during sleep in childhood, and nocturia is the undesired waking at night for micturition later in life. Studies show that at least 10% of school children have nocturnal enuresis[1,2], and 60–90% of the elderly over 60 years suffer from nocturia[3,4]. These conditions are detrimental to the quality of life by interfering with patients' self-esteem or sleeping habits, and they are the major diseases found in urology clinics. Nocturnal enuresis and nocturia are characterized by a mismatch between urine production rate in the kidneys and storage in the urinary bladder[5,6]. During the sound sleep of a healthy person, a smaller volume of urine is produced than that during the daytime, and more urine is stored during the sleep phase than during the active phase[7-9]. Although it is unknown how such temporal variation is generated, these phenomena could be related to biological rhythms because behaviour, physiology and metabolism in mammals are subject to a well-controlled daily rhythm, generated by an internal self-sustained molecular oscillator referred to as the circadian clock[10-13].

Circadian oscillations are driven by a transcription-translation feedback loop consisting of PER and CRY as negative components and CLOCK and BMAL1 as positive components. Rhythmic oscillations of this core loop are followed by the clock-associated oscillations of *Dbp* and *Rev-erbα*, whose products regulate oscillations

of a number of clock controlled genes regulating cell- or organ-specific physiology through D-box and RORE sites, respectively[14-16]. These molecular oscillators exist in most body cells and organs[13], but little is known about the role of the clock in urinary bladder function.

Micturition occurs by the contraction of smooth muscles of the urinary bladder upon a sensation of fullness, which is precisely controlled by regulation of the central and peripheral nerves[17,18]. We and others have reported that an increase in connexin43 (Cx43), a gap junction protein in the urinary bladder, enhances intercellular electrical and chemical transmission and sensitizes the response of bladder muscles to cholinergic neural stimuli. This results in a decrease in functional bladder capacity and an increase in micturition frequency in rats[19-22]. These phenomena mimic some aspects of an overactive bladder, a human pathological condition characterized by urinary urgency and increased micturition frequency[23]; however, the involvement of Cx43 in regulating normal bladder function remains unclear.

To further elucidate the role of Cx43 in bladder function, we investigated the effect of genetic ablation of *Cx43* on micturition behaviour in mice and the implication of *Cx43* for circadian micturition rhythm. The circadian micturition rhythm in free-moving mice still remains elusive, since the urine volume voided per micturition (UVVM) in

mice is so minute (sometimes <50 μl)[24,25]. To overcome this problem, we designed a novel system, called the automated voided stain on paper (aVSOP) method, which can accurately record micturition by mice for several days. Using this system, we demonstrated the role of *Cx43* and the circadian clock as regulators of functional bladder capacity in mice. We also showed that bladder muscle has internal rhythms of the clock and Cx43, which are correlated with oscillation in gap junction function. Further, we propose a novel paradigm that links the circadian clock with Cx43, in which Rev-erbα protein transactivates the *Cx43* promoter through interaction with Sp1.

RESULTS

Cx43 is involved in control of functional bladder capacity

We began our study by developing an automated machine called aVSOP (**Fig. 1a**). The conversion of UVVM by mice from a drop area on filter paper has been reported to be an accurate method[24,26], and this principle was applied to the automated system by using a laminated filter paper pre-treated to turn the edge of urine stains deep purple (**Supplementary Fig. S1a**). This modification enabled us to record the

micturition of free-moving mice fed *ad libitum* for several successive days, for a UVVM as little as 10 μl (**Supplementary Fig. S1b**).

To assess the effect of genetic *Cx43* ablation on micturition, we compared heterozygous $Cx43^{+/-}$ and wild-type (WT) $Cx43^{+/+}$ littermate mice by the aVSOP method (**Fig. 1b–d**) because homozygous $Cx43^{-/-}$ mice die shortly after delivery[27]. *Cx43* mRNA and protein levels in the urinary bladder of $Cx43^{+/-}$ mice were decreased compared with those in $Cx43^{+/+}$ mice (**Fig. 1e**,**f**). In both genotypes, UVVM showed temporal variation under 12-hour light and 12-hour dark (LD) conditions (**Fig. 1b–d**), consistent with the nocturnal characteristics of the mice[28]. UVVM was higher in $Cx43^{+/-}$ mice than that in $Cx43^{+/+}$ mice (**Fig. 1b–d)**, while total urine volume was not significantly different (**Supplementary Fig. S1c**).

These data demonstrate that the expression level of Cx43 is crucial for determining the functional capacity of the urinary bladder. This finding and the temporal variation in the micturition behaviour of the mice led us to focus on its association with *Cx43* expression in the bladder and the circadian clock.

Association of bladder clock with bladder capacity and *Cx43*

It has been reported that micturition shows a diurnal change in rodents as well

as in humans[8,22,28,29], although the day-night change is inverted because of the difference in diurnal versus nocturnal habits. However, it is unknown whether these changes are induced by an endogenous oscillator or only by a reflection of external light-dark changes. To address this in mice, we first examined micturition of WT mice under both LD and constant dark (DD) conditions. A distinct rhythm of UVVM was recorded, peaking at zeitgeber time (ZT) or circadian time (CT) 8–12 (**Fig. 2a,b**). Chi-square analysis showed a circadian periodicity under both LD and DD conditions (**Supplementary Fig. S2a**). No significant difference between LD and DD was found in the circadian amplitude (0.042 cycles per hour) quantified as relative power calculated by Fourier transform[30] (**Supplementary Fig. S2b**). This demonstrates that the mouse could be a model animal for micturition rhythmicity, and that the rhythm could be related to an internal biological rhythm that is also operational in the absence of environmental change in light/dark cycles. The involvement of the circadian clock in micturition behaviour was tested in mice with a dysfunctional circadian clock by deletion of *Cryptochrome-1* (*Cry1*) and *Cryptochrome-2* (*Cry2*) (*Cry*-null mice); accordingly, these mice have completely arrhythmic behaviour and metabolism[11,31]. We placed our aVSOP system in a box with an infrared activity sensor and measured the micturition and locomotor activity simultaneously. Similar to behavioural locomotor

rhythms (**Supplementary Fig. S3a**), circadian characteristics of UVVM observed in WT mice were abolished in *Cry*-null mice (**Fig. 2c,d**) analysed by Chi-square and Fourier transform (**Supplementary Fig. S3b**) as well as those of total urine volume and frequency (**Supplementary Fig. S3c,d**). These findings further support the notion that the circadian clock regulates UVVM.

We next examined whether the molecular machinery of the circadian clock is present in the urinary bladder. We found that the core oscillating machinery was present in the urinary bladder, as core clock genes including *Per2* and *Bmal1*(**Fig. 2e**), *Per1, Cry1, Clock* and *Dbp* (**Supplementary Fig. S4**) showed characteristic circadian expression profiles by real-time RT-PCR of circadian sampling of the urinary bladder every 4 hours (6 time points of the day) in WT mice. Dysfunction of the bladder circadian clock in *Cry*-null mice was demonstrated by a disturbed rhythm of *Per2* and *Bmal1* (**Fig. 2e**). We performed DNA microarray analysis to investigate the genes showing circadian rhythm in the urinary bladder more extensively. Besides the clock genes, there are thousands of oscillating genes in the bladder, as in other organs[32,33]. Notably, our target gene, *Cx43* (also known as *Gja1*), was among the 184 genes with clear circadian rhythmicity (defined as greater than the max correlation of 0.85 from the cosine curve with a 1.5-fold amplitude of expression level[34,35]) (**Supplementary Data**

1).

Cx43 mRNA showed a clear circadian rhythm with a peak at CT12 and a trough at CT0 by real-time RT-PCR (**Fig. 2f**). Cx43 protein levels remained low during the sleep phase (CT4–12), began to elevate 4 hours after the peak of mRNA expression, and formed a plateau during the active phase (CT16–24) (**Fig. 2g**). Immunostaining of Cx43 in the muscle layer of the urinary bladder at CT4 and at CT16 also showed a clear difference in immunoreactivity (**Fig. 2h**). In rats, in which day-night difference of micturition behaviour has been described[22,29], a similar correlation was observed between micturition rhythm (**Fig. 3a**), temporal variations of clock genes (*Per2* and *Bmal1*) and *Cx43* mRNA expressions in the urinary bladder (**Fig. 3b**), Cx43 protein levels (**Fig. 3c**) and Cx43 immunoreactivity (**Fig. 3d**).

The circadian change of mRNA was reflected in the protein level, and the increase/decrease in Cx43 protein expression correlated with the decrease/increase of UVVM, respectively, in WT mice and rats. Similarly, *Cry*-null mice tended to show a constantly low level of *Cx43* mRNA (**Fig. 2f**) with a high level of UVVM (**Fig. 2d**). This inverse expression can be accounted for by altered bladder sensitivity caused by a differential level of gap junction formation by Cx43 because the half-life of connexin proteins is up to 5 hours and expression largely follows transcript levels[36,37]. These

findings suggest that the bladder circadian clock coordinates UVVM via circadian regulation of *Cx43* gene expression.

Internal oscillations of bladder clock and Cx43 function

We investigated if the circadian clock oscillates in the bladder without systemic control. Therefore, we investigated its oscillation in *ex vivo* bladder in culture. We used mice carrying a PER2::LUC fusion protein, which has been engineered to produce bioluminescence when the clock gene *Per2* is activated in the presence of luciferin[38]. The *ex vivo* slice culture of the bladder from *Per2::luc* mice demonstrated a robust oscillation of bioluminescence in the muscle layer of the bladder for at least four cycles (**Fig. 4a** and **Supplementary Video 1**). The oscillation continued for approximately 2 months in the medium changed every 5 days. This oscillation was not observed in *Per2::luc* mice with the *Clock*-mutation ($Clk^{\Delta 19}/Clk^{\Delta 19}$) (**Supplementary Fig. S5**). These findings clearly demonstrate that a functional circadian clock exists in the smooth muscle of the urinary bladder.

We then examined cultured bladder smooth muscles cells (BSMC) under serum shock, an *in vitro* model of genetic oscillation[39]. After serum shock in BSMC, autonomous oscillation of clock genes (*Per2* and *Bmal1*) was observed (**Fig. 4b**).

Concurrently, *Cx43* levels also showed autonomous rhythmicity (**Fig. 4b**), which was followed by a change in protein levels (**Fig. 4c**,**d**), as observed in the bladder *in vivo* (**Figs. 2f–h** and **3b–d**). This change occurred in parallel with a change in cell-cell communication rate as shown by a dye-transfer experiment with lucifer yellow microinjected intracellularly (**Fig. 4e**). At 24 h after the initiation of rhythm when Cx43 protein levels were close to their nadir, the amount of dye-transferred cells was at its minimum. However, at 36 h when Cx43 protein levels were close to their peak, the amount of dye-transferred cells was considerably increased (more than 2-fold compared with the minimum level at 24 h). These findings clearly demonstrate that bladder muscle cells have an internal rhythm generating system, which elicits oscillation in gap junction function.

Activation of *Cx43* promoter by a clock component Rev-erbα

We next investigated the molecular mechanism of *Cx43* regulation by the clock. We searched for E-box, D-box and RORE sequences in the 5' prime region of *Cx43*, because clock genes are known to regulate clock-controlled genes by binding to these sequences[15,40,41]. However, we identified no such canonical sequences in a species-conserved manner within 10,000 bases from the transcription start site* (*for

RORE, there are 3 atypical RORE sequences detected from -720 to -467, but their transcriptional role for *Cx43* was negated as shown in **Supplementary Fig. S6** and **Supplementary Discussion**). Therefore, we suspected that the circadian clock might regulate the *Cx43* promoter by a novel mechanism.

We examined the effect of clock genes on the *Cx43* promoter by promoter-reporter assays in HEK293T cells using a pGL-2-mouse *Cx43*-promoter-reporter construct containing -1686/+165[42]. There was little effect of Clock/Bmal1 and Cry1 (positive and negative regulators of genes with E-box elements as shown for the *Per1* promoter) or of Dbp and E4bp4 (regulators of genes with D-box elements as shown for the *Per1* promoter) on the *Cx43* promoter (**Supplementary Fig. S7a,b**). A RORE-binding protein, Rorα, also did not have any effect on *Cx43* promoter activity. However, Rev-erbα, which has been reported as a negative competitor of Rorα[43] (as shown for the *Bmal1* promoter, **Supplementary Fig. S7c**), markedly increased *Cx43* promoter activity (**Supplementary Fig. S7a**) in a dose-dependent manner (**Fig. 5a**), while the application of various concentrations of a mutant Rev-erbα (Rev-erbα truncated mutant deleted with 127–206 amino acids) failed to activate the *Cx43* promoter (**Fig. 5b**).

Additionally, in BSMC, Rev-erbα dose-dependently upregulated *Cx43*

promoter activity (**Fig. 5c**). Conversely, inhibition of Rev-erbα by siRNA decreased Cx43 mRNA and protein expression (**Fig. 5d**), while the same siRNA enhanced expression of Bmal1. These results suggest that *Cx43* activation is elicited through an unreported positive transcriptional control by Rev-erbα. *Rev-erbα* mRNA showed a clear circadian rhythm in mouse and rat urinary bladders with a peak time at CT/ZT 4–12 and a trough at CT/ZT16–24 (**Fig. 5e,f**). In *Cry*-null mice, *Rev-erbα* mRNA stayed arrhythmic at a lower level (**Fig. 5e**). These two patterns are consistent with the role of Rev-erbα as a positive regulator for *Cx43*, because the *Cx43* expression profile showed a peak at CT/ZT12–20 and a trough at CT/ZT0–8 in WT mice and rats, but stayed arrhythmic at a lower level in *Cry*-null mice (**Figs. 2f** and **3b**).

Sp1 dependent activation of *Cx43* transcription by Rev-erbα

To clarify the novel molecular mechanism of Rev-erbα on promoter activity, we first attempted to identify the site with effects on the *Cx43* promoter by a deletion experiment because the 5' region of *Cx43* contains several *cis*-elements including AP-1, AP-2, Sp1, half ERE, and cAMP-response element[44]. Truncated -700/+165, -300/+165 and -147/+165 constructs did not affect the activation of the *Cx43* promoter by Rev-erbα. In contrast, the transcription activation of *Cx43* by Rev-erbα was markedly

diminished in the -54/+165 and -44/+165 constructs (**Fig. 6a**).

Between -147 and -54 of the *Cx43* promoter, there are *cis*-elements evolutionally conserved among humans, rats and mice including three putative GC-rich Sp1-binding sites (**Fig. 6b**)[45,46]. Exogenous expression of a transcription factor Sp1 activated the *Cx43* promoter in a dose-dependent manner, and its effect was dramatically increased by the addition of exogenous Rev-erbα (**Fig. 6c**). Protein expression of Cx43 was also upregulated by exogenous Sp1 and Rev-erbα (**Fig. 6d**). The promoter activation induced by Sp1/Rev-erbα was inhibited by mutations of the three Sp1 *cis*-elements, in which the proximal was most crucial (Sp1C in **Fig. 6e**), and was completely abolished by deletion of all Sp1 sites (**Fig. 6e**). Sp3, another activator bound to Sp1 sites of *Cx43* promoter[45], also enhanced *Cx43* promoter activity in the presence of Rev-erbα (**Supplementary Fig. S8**), supporting the involvement of Sp1 sites for enhancement of *Cx43* transcription by Rev-erbα.

In conclusion, unlike the negative transcriptional role of Rev-erbα using RORE sites, the novel positive transcriptional role of Rev-erbα requires Sp1 *cis*-elements on the *Cx43* promoter.

Rhythmic assembly of Rev-erbα and Sp1 at *Cx43* promoter

We hypothesized that Rev-erbα acts as a co-factor of Sp1, because Rev-erbα dose-dependently enhanced *Cx43* activation by Sp1. To determine whether Rev-erbα interacts with Sp1 at Sp1 sites of the *Cx43* promoter, a co-immunoprecipitation assay and chromatin immunoprecipitation assay (ChIP) were performed in HEK293T cells transfected with HA-Rev-erbα and DDDDK-Sp1 (protein expression of these constructs are shown in **Supplementary Fig. S9**). We observed a DDDDK-Sp1 band in immunoprecipitates with an anti-HA antibody, and HA-Rev-erbα was detected in immunoprecipitates with an anti-DDDDK antibody (**Fig. 7a**), indicating that Rev-erbα can form a complex with Sp1. The ChIP assay revealed that, in immunoprecipitates of the chromatin fragments using antibodies for HA and DDDDK, specific enrichment was obtained by primers targeted on Sp1 *cis*-elements of the human *Cx43* promoter (**Fig. 7b**). These findings demonstrate that Rev-erbα interacts with Sp1 at Sp1 sites of the *Cx43* promoter.

We next examined whether the endogenous Rev-erbα/Sp1 complex is rhythmically formed on Sp1 sites of the *Cx43* promoter. It is likely that Rev-erbα, but not Sp1, could contribute to the rhythmic formation of the Rev-erbα/Sp1 complex, because *Sp1* mRNA showed no marked rhythm (**Fig. 7c**), in contrast with the strong rhythm of *Rev-erbα* mRNA in the bladder (**Fig. 5e,f**). To verify the rhythmic role of

Rev-erbα estimated *in vivo*, we applied rat BSMC under serum shock *in vitro* for the ChIP assay on the *Cx43* promoter using an anti-Rev-erbα antibody. After confirming the circadian expression of *Rev-erbα* mRNA and protein (**Fig. 7d**), we harvested the cells before serum shock and 14 h and 26 h after serum shock. A higher level of Rev-erbα was detected on Sp1 sites of the *Cx43* promoter at 26 h, when *Cx43* mRNA expression showed a peak, than that at 14 h when *Cx43* mRNA expression was at the nadir (**Fig. 4b**). Therefore, we conclude that this rhythmic formation of the Rev-erbα/Sp1 complex on the Sp1 sites of *Cx43* promoter is one mechanism that the clock induces for circadian oscillation of *Cx43* expression (**Fig. 7e**).

DISCUSSION

Day-night micturition rhythm in humans enables a sound sleep during the sleep phase. This rhythm is not simply caused by a higher water intake during the day, because temporal variation in urine production is maintained in subjects under constant routine, when food and drink are taken equally during 24 hours[47]. In physiological conditions, nocturnal micturition is prevented not only by a decrease in urine

production rate from the kidneys, but also by an increase in storage capacity of the urinary bladder[7-9]. Day-night differences in bladder capacity are experienced in the daily life of humans and their disturbance can be seen in disorders such as nocturnal enuresis and nocturia. The treatment of these patients in clinics is often limited to palliation because the precise mechanism underlying the micturition rhythm is unknown.

In the beginning of the current study, we aimed to use a mouse model with/without genetic modification for investigating this mechanism. A day-night difference in micturition is known to exist in humans and rodents[8,22,28,29], but circadian analysis of micturition in mice has been precluded by the difficulty in diachronic measuring of urine volume with high accuracy. To overcome these problems, we designed the aVSOP system, which enabled an accurate record of minute micturition volume as little as 10 μl for several days. This method clearly recorded circadian rhythm of micturition in mice (also avoiding micturition during the sleep phase), suggesting that this rhythm should have a mechanism conserved among species. The aVSOP method also enabled us to use genetically engineered mice for unravelling the molecular events responsible for controlling micturition. In *Cx43*$^{+/-}$ mice, this method showed the importance of Cx43 for determining functional bladder capacity, and in *Cry*-null mice,

it showed a novel function of the circadian clock: circadian regulation of functional bladder capacity. Oscillation of the internal clock was demonstrated in the urinary bladder muscle layer *ex vivo* and in cultured BSMC, in parallel with the functional change in gap junctions, compatible with the rhythm of Cx43 levels. Collectively, these findings constitute the key concept of this study: the clock elicits oscillation in Cx43 levels and sensitivity of BSMC, which contribute to altered functional bladder capacity and micturition frequency during the 24 hour cycle.

Micturition during the sleep phase is undesirable for humans, in terms of arousal from sleep, hygiene or maintenance of body temperature, which could also be applicable to rodents. By focusing on Cx43 in the urinary bladder and the circadian clock in the present study, we showed a novel aspect in normal and pathological physiology of the diurnal micturition rhythm. However, we should also note that Cx43 in the bladder is not the only determinant of this rhythm. Enuresis and nocturia are caused not only by decreased functional bladder capacity, but also by impairment of cortical arousal level in the brain, urine production rhythm in the kidneys[4], and interaction between each other[48]. In the bladder, there are also many other candidate molecules with diurnal oscillation, as listed in our microarray data (**Supplementary Data 1**), such as genes associated with smooth muscle contraction (*Cacna1g, Ednrb* and

Gucy1a3) or response to pain (*Slc6a2*, *Ednrb* and *Grik1*). These genes could also be contributing to micturition rhythm. Future studies may elucidate the association of these factors with the circadian clock, and the aVSOP method could serve as an important tool for that purpose.

The molecular mechanism of *Cx43* oscillation that may underlie these phenomena is also noteworthy. Rev-erbα protein, known as a constitutive repressor[43,49], acts as a transcriptional activator for *Cx43* by luciferase-reporter assay. Intriguingly, for *Cx43* activation, Rev-erbα does not require a canonical RORE site, but acts indirectly on Sp1 sites by interacting with Sp1 protein. This is similar to previous reports showing the physical interaction of Sp1 and nuclear receptors, such as RAR, RXR, ERs and PPARγ[50-52]. The identification of a co-activator-like function of Rev-erbα advocates a novel paradigm for controlling circadian gene expression: circadian clock components can modulate the activity of transcription factors coded by non-clock genes by functioning as transcriptional co-factors. Genome-wide screening of putative clock-associated sequences has revealed that many genes showing circadian oscillation do not have binding sequences for clock proteins[14,15], and our finding suggests that these genes could possibly be regulated by clock proteins acting as co-factors.

In summary, the circadian clock is associated with the oscillating expression of Cx43 in BSMC via a previously unknown regulatory mechanism, and it contributes to changes in bladder capacity with an increase during the sleep phase and a decrease during the active phase. This study warrants chronobiological approaches for the investigation and treatment of nocturnal enuresis and nocturia.

METHODS

Animals. Female *Cx43* heterozygote KO mice (*Cx43*$^{+/-}$)[53] aged 16-21 weeks, their female WT littermates (*Cx43*$^{+/+}$), and female *Cry1*$^{-/-}$*Cry2*$^{-/-}$ mice (*Cry*-null)[11] aged 10 weeks were used. C57BL/6 mice and Sprague-Dawley (SD) female rats were purchased from Japan Lab Animals Co., Ltd and Japan SLC. Animals were treated in accordance with NIH animal care guidelines, and the Kyoto University Animal Experiment Committee approved all animal experiments.

Micturition analysis in mice. Micturition assessment machines for aVSOP were manufactured by Real-designs Co., Ltd (Kyoto, Japan). Rolled laminated filter paper, pre-treated to turn the edge of urine stains deep purple, was wound up at a speed of 10 cm/h under a water-repellent wire lattice. Urine stains were counted and traced to convert micturition volume by the formula of a standard curve, calculated by the correlation of normal saline and the stained area ranging from 10 to 800 μl. *Cx43*$^{+/-}$ and *Cx43*$^{+/+}$ mice were kept in a cage with the dimensions of 110×160×75 mm (height × depth × width), measured under LD conditions for 4 days and sacrificed for RNA extraction. The male WT mice were measured for 8 days under LD and followed by 5 days under DD conditions. The female WT and *Cry*-null mice were kept in a cage with

dimensions of 75×160×75 mm, and measured with a simultaneous actogram under DD conditions for 5 days. Total urine volume per hour was estimated by dividing the volume by the time interval between the given and preceding voiding (filling time) when the filling time was more than 1 hour[7].

Micturition analysis in rats. Micturition of SD rats was recorded by an electronic balance system[22] under LD conditions for 2 days.

Real-time RT-PCR analysis. Female C57BL/6 mice aged 8 weeks and *Cry*-null mice aged 10 weeks were sacrificed every 4 hours at six time points during the day under a dim light (n=3 for each time/strain) after acclimation for 2 weeks under LD conditions followed by DD conditions. Female SD rats aged 7 weeks were acclimated for a week under LD conditions and sacrificed at every 4 hours (n=5 for each time), followed by DD conditions, and then sacrificed in the same manner (n=2 for each time). Complementary DNA was synthesized from 1 μg of RNA extracted from the bladder and cultured cells using a Superscript VILO cDNA Synthesis Kit (Invitrogen). Primers used are listed in **Supplementary Table S1**. Real-time RT-PCR was performed using SYBR Green PCR Master Mix with 7500 Fast Real-Time PCR system (Applied

Biosystems)[22]. Each sample was normalized against an internal 18s ribosomal RNA control (Takara). Maximal correlation coefficients (MaxCorr) were calculated using Mathematica ver. 5.1 according to a modified program[35].

Immunoblotting. Whole cell lysates from bladder tissues and cultured cells were lysed with radioimmunoprecipitation assay (RIPA) buffer containing proteinase inhibitors, which were resolved by SDS-PAGE and transferred to an Immobilon-P membrane. The membranes were incubated with antibodies against Cx43 (Zymed, 1:200; Sigma-Aldrich, 1:1000), Rev-erbα (Cell Signaling Technology [CST], 1:500; Abcam, 1:600), Bmal1 (Santa Cruz, 1:200), Sp1 (Millipore, 1:2000), αSMA (Sigma-Aldrich, 1:5000), Sp3 (BioLegend, 1:500), HA (Abcam, 1:8000), DDDDK (MBL, 1:2000) and GAPDH (CST, 1:2000). The immunoreactivities were visualized with enhanced chemiluminescence using HRP-conjugated anti-rabbit or mouse IgG antibody (Pierce)[22].

Bioluminescence recording. Slice cultures of bladder were obtained from adult *Period2*^{Luciferase} knock-in (*Per2::luc*) mice[38] (Jackson Laboratories), and *Per2::luc* mice with a *Clock* mutation (*Clk*$^{\Delta 19}$/*Clk*$^{\Delta 19}$) generated by crossing *Per2::luc* mice to *Clock*

mutant ($Clk^{\Delta 19}/Clk^{\Delta 19}$) mice (Jackson Laboratories). The slice cultures were kept at 36°C with culture medium containing 1 mM luciferin[54]. Bioluminescence was measured with a highly sensitive cryogenic CCD camera (Spectra Video SV16KV/CT; Pixelvision) equipped with a microscope (Carl Zeiss)[55].

Immunostaining of the urinary bladder. Mice bladder tissues and slice cultures were fixed with 4% paraformaldehyde in 0.1M phosphate buffer (0.1MPB, pH 7.4) for 24 hours[54]. After embedding bladder tissues in paraffin, we cut 5 μ thick sections with a microtome. After being treated with 1% BSA, sections were incubated with Cx43 rabbit polyclonal antibody (Invitrogen, 1:50) or αSMA (Sigma-Aldrich, 1:400). Immunoreactions were visualized by donkey anti-rabbit Alexa 594 (Molecular Probes), and observed by a fluorescent microscope (Carl Zeiss).

Serum shock analysis of BSMC. Primary BSMC, isolated from female SD rats aged 9 weeks[22,56], were cultured after two passages until sub-confluent in DMEM with 10% FCS and 1% penicillin streptomycin followed by 72 hours incubation in DMEM with 0.5% FCS. The cells were treated with 50% horse serum (GIBCO-BRL) in DMEM for 2 hours[39], and washed twice with DMEM and then maintained in DMEM with 0.5% of

FCS for a maximum of 72 hours.

Immunostaining of BSMC. BSMC were serum-shocked and fixed with 4% formaldehyde, permeabilized with 0.4% Triton X-100, and blocked with 10% goat serum (Invitrogen). The cells were incubated with Cx43 rabbit polyclonal antibody (Sigma-Aldrich, 1:500) followed by goat anti-rabbit Alexa 594 (Molecular Probes) and counter stained with DAPI[57].

Lucifer yellow microinjections. Nuclei of serum-shocked BSMC were pre-stained by 16 μM of Hoechst 33342 (Invitrogen) for 15 minutes to identify the site of injection. A single cell was impaled with a microelectrode and Lucifer Yellow was injected by an electrometer (model 3100; A-M systems) for 1 minute with a continuous current of 0.1 μA. Images were acquired using a CoolSNAP-HQ2 CCD camera (Photometrics)[57]. Fluorescent cells were counted and the values were normalized by the total number of cells within the injected region of interest (ROI), with a mean cell density of 32.6 ± 6.6 cells).

Promoter-reporter assay. The promoter-reporter constructs used were, mouse pGL-2-Cx43 (pCx43 -1686/+165-luc)[42], mouse pGL-3-Per1 (pPer1-luc),

pGL-3-Bmal1 (pBmal1-luc), and pGL-2 basic, pRL-TK (Promega) as controls. The expression vectors used were, Sp1 and Sp3 (fully lengthened according to a previous report)[58, 59], Clock, Bmal1, Cry1, Dbp, E4bp4, Rev-erbα and Rorα (Open Biosystems). Site-directed mutagenesis, deletion and addition of aimed sequences were performed using a mutagenesis basal kit (Takara). Corrected mutants were all verified by sequencing. For luciferase assays, reporter plasmids (100 ng) with various expression vectors (total 250 ng) were transfected to HEK293T cells in 24-well plates and those (total 100 ng) to BSMC in 96-well plates using Fugene6 (Roche) in DMEM with 10% FCS. Plasmid dosage was kept constant by the EGFP-N1 vector. Lysates were harvested 48 hours post-transfection, and the luciferase activity was measured using a dual luciferase assay reagent (Promega).

RNA interference assay. Three sets of Stealth Select RNAi targeted against rat Rev-erbα (Rat Nr1d1 1330003) and Stealth RNAi Negative Control (low, medium and high GC, Invitrogen) were used. After two passages, BSMC were plated on 6-well plates and kept for 24 hours in DMEM with 10% FCS. This was followed by transfection of siRNA (75 pmol/well) in serum-reduced αMEM for 5 hours using Lipofectamin RNAiMAX (Invitrogen), followed by medium-change to DMEM with 10% FCS. After 48 hours of the transfection, total RNA and cell lysates were extracted.

Co-immunoprecipitation assay. Rev-erbα with N-terminal MYPYDVPDYA-tag

(HA-Rev-erbα) and Sp1 with N-terminal MDYKDDDDK-tag (DDDDK-Sp1) were constructed using a mutagenesis basal kit (Takara). Nuclear extracts were prepared from HEK293T cells transfected with expression vectors for 48 hours, using a Nuclear Complex Co-IP kit (Active Motif,). A total of 100 μg of nuclear extracts were incubated with antibodies for 0.27 μg of Rev-erbα (CST), 4 μg of HA (Abcam), DDDDK (MBL) and control rabbit IgG (Zymed), in 500 μl of low IP buffer overnight at 4°C with rotation followed by the addition of 30 μl of Dynabeads Sheep anti-Rabbit IgG (Veritas) for 1 hour. After washing with low IP buffer with/without BSA three times each, the binding protein was eluted in 40 μl of RIPA buffer for immunoblotting. A total of 2 μg of nuclear extracts were used as input.

Chromatin immunoprecipitation. Formaldehyde-cross-linked chromatins were obtained from HEK293T cells and serum-shocked BSMC, which were sheared using Chip-IT Express Enzymatic (Active Motif). Sheared chromatins were immunoprecipitated with antibodies to 0.23 μg of Rev-erbα (Lifespan Biosciences, LS-C37817), 2 μg of HA, DDDDK and control rabbit IgG overnight at 4°C with rotation followed by the addition of 15 μl of Dynabeads Sheep anti-Rabbit IgG for 1 hour. The Chip-IT control kits Rat and Human (Active Motif) were used as an

experimental control. The enrichment of Sp1-binding sequences in eluted DNA was de-crosslinked by incubation at 65°C for 4 hours followed by digestion of protein by proteinase K. Purified DNA, using a QIAquick PCR purification kit (Qiagen), was quantified by real-time RT-PCR and normalized by the quantity of input DNA[60]. Samples of BSMC after real-time RT-PCR were visualized by electrophoresis. Primers used are listed in **Supplementary Table S1**.

Statistical analysis. For the micturition experiments, we used one-way ANOVA with Bonferroni's *post hoc* test to evaluate differences among time points. Two-way repeated measures ANOVA was used to compare differences between the two groups of mice tested, and time points were compared with Bonferroni's *post hoc* test. For the experiments in which three or more test groups were compared, we used one-way ANOVA, and for those including two factors, we used two-way ANOVA.

Additional methods. Microarray analysis is described in the Supplementary Methods. Microarray data has been deposited in the Gene Expression Omnibus under accession code GSE35795.

REFERENCES

1. Robson WL. Clinical practice. Evaluation and management of enuresis. *N Engl J Med* **360,** 1429-1436 (2009).
2. Neveus T. Diagnosis and management of nocturnal enuresis. *Curr Opin Pediatr* **21,** 199-202 (2009).
3. Bosch JL & Weiss JP. The prevalence and causes of nocturia. *J Urol* **184,** 440-446 (2010).
4. van Kerrebroeck P et al. The standardisation of terminology in nocturia: report from the Standardisation Sub-committee of the International Continence Society. *Neurourol Urodyn* **21,** 179-183 (2002).
5. Van Hoeck K et al. Urine output rate and maximum volume voided in school-age children with and without nocturnal enuresis. *J Pediatr* **151,** 575-580 (2007).
6. Weiss JP, Blaivas JG, Stember DS & Chaikin DC. Evaluation of the etiology of nocturia in men: the nocturia and nocturnal bladder capacity indices. *Neurourol Urodyn* **18,** 559-565 (1999).
7. Van Hoeck K, Bael A, Lax H, Hirche H & van Gool JD. Circadian variation of

voided volume in normal school-age children. *Eur J Pediatr* **166,** 579-584 (2007).

8. Nakamura S et al. Circadian changes in urine volume and frequency in elderly men. *J Urol* **156,** 1275-1279 (1996).
9. Witjes WP, Wijkstra H, Debruyne FM & de la Rosette JJ. Quantitative assessment of uroflow: is there a circadian rhythm? *Urology* **50,** 221-228 (1997).
10. Reppert SM & Weaver DR. Coordination of circadian timing in mammals. *Nature* **418,** 935-941 (2002).
11. Doi M et al. Salt-sensitive hypertension in circadian clock-deficient Cry-null mice involves dysregulated adrenal Hsd3b6. *Nat Med* **16,** 67-74 (2010).
12. Takahashi JS, Hong HK, Ko CH & McDearmon EL. The genetics of mammalian circadian order and disorder: implications for physiology and disease. *Nat Rev Genet* **9,** 764-775 (2008).
13. Dibner C, Schibler U & Albrecht U. The mammalian circadian timing system: organization and coordination of central and peripheral clocks. *Annu Rev Physiol* **72,** 517-549 (2010).
14. Panda S et al. Coordinated transcription of key pathways in the mouse by the circadian clock. *Cell* **109,** 307-320 (2002).
15. Ueda HR et al. System-level identification of transcriptional circuits underlying

mammalian circadian clocks. *Nat Genet* **37,** 187-192 (2005).

16. Okamura H, Doi M, Fustin JM, Yamaguchi Y & Matsuo M. Mammalian circadian clock system: Molecular mechanisms for pharmaceutical and medical sciences. *Adv Drug Deliv Rev* **62,** 876-884 (2010).

17. Birder L et al. Neural control of the lower urinary tract: peripheral and spinal mechanisms. *Neurourol Urodyn* **29,** 128-139 (2010).

18. Andersson KE. Antimuscarinic Mechanisms and the Overactive Detrusor: An Update. *Eur Urol.* **59,** 377-386 (2010).

19. Imamura M et al. Basic fibroblast growth factor causes urinary bladder overactivity through gap junction generation in the smooth muscle. *Am J Physiol Renal Physiol* **297,** F46-F54 (2009).

20. Christ GJ et al. Increased connexin43-mediated intercellular communication in a rat model of bladder overactivity in vivo. *Am J Physiol Regul Integr Comp Physiol* **284,** R1241-1248 (2003).

21. Suadicani SO, Urban-Maldonado M, Tar MT, Melman A & Spray DC. Effects of ageing and streptozotocin-induced diabetes on connexin43 and P2 purinoceptor expression in the rat corpora cavernosa and urinary bladder. *BJU Int* **103,** 1686-1693 (2009).

22. Negoro H et al. Regulation of connexin 43 by basic fibroblast growth factor in the bladder: transcriptional and behavioral implications. *J Urol* **185,** 2398-2404 (2011).

23. Haferkamp A et al. Increased expression of connexin 43 in the overactive neurogenic detrusor. *Eur Urol* **46,** 799-805 (2004).

24. Sugino Y et al. Voided stain on paper method for analysis of mouse urination. *Neurourol Urodyn* **27,** 548-552 (2008).

25. Wood R, Eichel L, Messing EM & Schwarz E. Automated noninvasive measurement of cyclophosphamide-induced changes in murine voiding frequency and volume. J Urol **165,** 653-659 (2001).

26. Birder LA et al. Altered urinary bladder function in mice lacking the vanilloid receptor TRPV1. *Nat Neurosci* **5,** 856-860 (2002).

27. Reaume AG et al. Cardiac malformation in neonatal mice lacking connexin43. *Science* **267,** 1831-1834 (1995).

28. Bassuk JA, Grady R & Mitchell M. Review article: The molecular era of bladder research. Transgenic mice as experimental tools in the study of outlet obstruction. *J Urol* **164,** 170-179 (2000).

29. Herrera GM & Meredith AL. Diurnal variation in urodynamics of rat. *PLoS One* **5**,

e12298 (2010).

30. Meredith AL et al. BK calcium-activated potassium channels regulate circadian behavioral rhythms and pacemaker output. *Nat Neurosci* **9,** 1041-1049 (2006).

31. van der Horst GT et al. Mammalian Cry1 and Cry2 are essential for maintenance of circadian rhythms. *Nature* **398,** 627-630 (1999).

32. Storch KF et al. Extensive and divergent circadian gene expression in liver and heart. *Nature* **417,** 78-83 (2002).

33. Hoogerwerf WA et al. Transcriptional profiling of mRNA expression in the mouse distal colon. *Gastroenterology* **135,** 2019-2029 (2008).

34. McDonald MJ & Rosbash M. Microarray analysis and organization of circadian gene expression in Drosophila. *Cell* **107,** 567-578 (2001).

35. Yamada R & Ueda HR. Microarrays: statistical methods for circadian rhythms. *Methods Mol Biol* **362,** 245-264 (2007).

36. Fallon RF & Goodenough DA. Five-hour half-life of mouse liver gap-junction protein. *J Cell Biol* **90,** 521-526 (1981).

37. Bennett MV et al. Gap junctions: new tools, new answers, new questions. *Neuron* **6,** 305-320 (1991).

38. Yoo SH et al. PERIOD2::LUCIFERASE real-time reporting of circadian

dynamics reveals persistent circadian oscillations in mouse peripheral tissues. *Proc Natl Acad Sci U S A* **101,** 5339-5346 (2004).

39. Balsalobre A, Damiola F & Schibler U. A serum shock induces circadian gene expression in mammalian tissue culture cells. *Cell* **93,** 929-937 (1998).

40. Mitsui S, Yamaguchi S, Matsuo T, Ishida Y & Okamura H. Antagonistic role of E4BP4 and PAR proteins in the circadian oscillatory mechanism. *Genes Dev* **15,** 995-1006 (2001).

41. Preitner N et al. The orphan nuclear receptor REV-ERBalpha controls circadian transcription within the positive limb of the mammalian circadian oscillator. *Cell* **110,** 251-260 (2002).

42. Chen ZQ et al. Identification of two regulatory elements within the promoter region of the mouse connexin 43 gene. *J Biol Chem* **270,** 3863-3868 (1995).

43. Ueda HR et al. A transcription factor response element for gene expression during circadian night. *Nature* **418,** 534-539 (2002).

44. Oyamada M, Oyamada Y & Takamatsu T. Regulation of connexin expression. *Biochim Biophys Acta* **1719,** 6-23 (2005).

45. Teunissen BE et al. Analysis of the rat connexin 43 proximal promoter in neonatal cardiomyocytes. *Gene* **322,** 123-136 (2003).

46. Echetebu CO, Ali M, Izban MG, MacKay L & Garfield RE. Localization of regulatory protein binding sites in the proximal region of human myometrial connexin 43 gene. *Mol Hum Reprod* **5,** 757-766 (1999).

47. Boivin DB, Duffy JF, Kronauer RE & Czeisler CA. Sensitivity of the human circadian pacemaker to moderately bright light. *J Biol Rhythms* **9,** 315-331 (1994).

48. Yeung CK, Diao M & Sreedhar B. Cortical arousal in children with severe enuresis. *N Engl J Med* **358,** 2414-2415 (2008).

49. Yin L & Lazar MA. The orphan nuclear receptor Rev-erbalpha recruits the N-CoR/histone deacetylase 3 corepressor to regulate the circadian Bmal1 gene. *Mol Endocrinol* **19,** 1452-1459 (2005).

50. Suzuki Y et al. Physical interaction between retinoic acid receptor and Sp1: mechanism for induction of urokinase by retinoic acid. *Blood* **93,** 4264-4276 (1999).

51. Shimada J et al. Transactivation via RAR/RXR-Sp1 interaction: characterization of binding between Sp1 and GC box motif. *Mol Endocrinol* **15,** 1677-1692 (2001).

52. Sun G, Porter W & Safe S. Estrogen-induced retinoic acid receptor alpha 1 gene expression: role of estrogen receptor-Sp1 complex. *Mol Endocrinol* **12,** 882-890

(1998).

53. Suadicani SO, Brosnan CF & Scemes E. P2X7 receptors mediate ATP release and amplification of astrocytic intercellular Ca2+ signaling. *J Neurosci* **26,** 1378-1385 (2006).

54. Yamaguchi S et al. Synchronization of cellular clocks in the suprachiasmatic nucleus. *Science* **302,** 1408-1412 (2003).

55. Doi M et al. Circadian regulation of intracellular G-protein signalling mediates intercellular synchrony and rhythmicity in the suprachiasmatic nucleus. *Nat Commun* **2**, 327 (2011).

56. Wang HZ, Brink PR & Christ GJ. Gap junction channel activity in short-term cultured human detrusor myocyte cell pairs: gating and unitary conductances. *Am J Physiol Cell Physiol* **291,** C1366-C1376 (2006).

57. Thi MM, Urban-Maldonado M, Spray DC & Suadicani SO. Characterization of hTERT-immortalized osteoblast cell lines generated from wild-type and connexin43-null mouse calvaria. *Am J Physiol Cell Physiol* **299,** C994-C1006 (2010).

58. Hagen G, Muller S, Beato M & Suske G. Sp1-mediated transcriptional activation is repressed by Sp3. *EMBO J* **13,** 3843-3851 (1994).

59. Sapetschnig A, Koch F, Rischitor G, Mennenga T & Suske G. Complexity of translationally controlled transcription factor Sp3 isoform expression. *J Biol Chem* **279,** 42095-42105 (2004).

60. Kanematsu A, Ramachandran A & Adam RM. GATA-6 mediates human bladder smooth muscle differentiation: involvement of a novel enhancer element in regulating alpha-smooth muscle actin gene expression. *Am J Physiol Cell Physiol* **293,** C1093-1102 (2007).

ACKNOWLEDGEMENTS

We thank D.C. Spray, A. Mello, M.M. Thi, M. Tanaka, R. Matsuoka, Y. Kimura, N. Kawakami, Y. Sugino, T. Kobayashi, Y. Kajita, S.J. Lye, J. Yao, G. Suske, J. Toguchida, M. Yamamoto, S. Karki, J.M. Fustin and A. Negoro. This work was supported by a Grant-in-Aid for Scientific Research (20390425, 21390439, 23659756 and 18002016) from the Japan Society for the Promotion of Science, a grant from the National Institutes of Health (DK 081435), a grant from the Translational Research Centre in Kyoto University, an Asahi Kasei Pharma Urological Academy Grant, the Suzuki Urological Foundation and the Kyoto University Foundation.

AUTHOR CONTRIBUTIONS

H.N. and A.K. designed the experiments, analysed data and prepared the manuscript. H.N. performed most of the experiments. M.D. and H.O. contributed to the study design and manuscript preparation. S.O.S. provided *Cx43*$^{+/-}$ mice and contributed to the microinjection of Lucifer yellow. M.M. contributed to the analysis of rhythm-associated experiments. M.I., T. Okinami, N.N., K.S., M.T. and S.U. helped with *in vitro* experiments. T. Oura and S.M. analysed microarray data. E.M. contributed to morphological analysis. T.T. provided *Cry*-null mice. H.O., Y.T. and O.O. supervised the study.

COMPETING FINANCIAL INTERESTS

The authors declare no competing financial interests.

LEGENDS

Figure 1 AVSOP method reveals an association between functional bladder capacity and the *Cx43* gene. (**a**) A photograph and diagram showing the aVSOP method. Each stain was traced, scanned and quantified by Image J 1.42 software. (**b-d**) Female *Cx43*$^{+/-}$ mice had larger functional bladder capacity than sex-matched *Cx43*$^{+/+}$ littermates. (**b**) A photograph of urine spots on paper made by *Cx43*$^{+/+}$ (upper) and *Cx43*$^{+/-}$ (lower) mice. The scale bar indicates 10 cm, corresponding to 1 hour. (**c**) Representative charts of UVVM of *Cx43*$^{+/+}$ (upper) and *Cx43*$^{+/-}$ (lower) mice under light/dark conditions for 4 days. UVVM, urine volume voided per micturition. (**d**) UVVM per 6 hours in *Cx43*$^{+/+}$ and *Cx43*$^{+/-}$ mice had diurnal variation (F(3[degrees of freedom (DF) for the time factor],9[error DF])=12.3 and 10.9, respectively; **P* < 0.005 by one-way repeated measures ANOVA; #*P* < 0.05 in the late light [sleep] phase vs. late dark [active] phase, followed by Bonferroni's *post hoc* test). Maximal correlations from a cosine curve (MaxCorr) of *Cx43*$^{+/+}$ and *Cx43*$^{+/-}$ mice were 0.949 and 0.989, respectively. ZT, zeitgeber time: light-on at ZT0 and off at ZT12. UVVM was significantly different between *Cx43*$^{+/+}$ and *Cx43*$^{+/-}$ mice (F(1[DF for the strain factor],6[error DF])=11.2, *P* < 0.05 by two-way repeated measures ANOVA; †*P* < 0.05 vs. *Cx43*$^{+/+}$ by Bonferroni's *post hoc* test; n=4 for each group, with a total of 296

micturitions). Error bars represent s.e.m.. (**e**) Relative *Cx43* mRNA levels of the urinary bladder in $Cx43^{+/-}$ and $Cx43^{+/+}$ mice used in the micturition analysis by real-time RT-PCR. Error bars represent s.d., n=4 for each mice. The value of $Cx43^{+/+}$ was set as 1. *$P < 0.05$ by Student's *t*-test. (**f**) Cx43 protein expression of the urinary bladder in $Cx43^{+/+}$ and $Cx43^{+/-}$ mice.

Figure 2 Rhythmicity of micturition, clock genes and *Cx43* expression in wild-type mice is disturbed in *Cry*-null mice. (**a**) A representative chart of UVVM of WT C57BL/6 mice under LD conditions followed by DD conditions. (**b**) Temporal UVVM every 4 hours in WT mice (n=5), for 8 days under LD conditions (940 micturitions) and 5 days under DD conditions (556 micturitions). Diurnal variation of UVVM in LD conditions ($F(5,20)=17.28$, $^{**}P < 0.005$ by one-way repeated measures ANOVA) was also observed in DD conditions ($F(5,20)=8.23$, $^{*}P < 0.05$), with no significant difference among times in LD vs. DD by two-way repeated measures ANOVA. (**c, d**) There was a loss of circadian rhythm of UVVM in *Cry*-null mice under DD conditions. Age-matched female WT, 1493 micturitions; *Cry*-null, 1009 micturitions, n=5 each. (**c**) A representative chart of UVVM of *Cry*-null mice. (**d**) Temporal UVVM every 4 hours in *Cry*-null (red-diamond) and WT (black-diamond) mice. Diurnal variation detected in WT mice ($F(5,20)=8.21$, $P < 0.05$ by one-way repeated measures ANOVA) was not observed in *Cry*-null mice. (**e**) Temporal *Per2*, *Bmal1* and (**f**) *Cx43* mRNA accumulation in the bladder in WT and *Cry*-null mice (n=3 for each time point). MaxCorrs of *Per2*, *Bmal1* and *Cx43* were (0.96, 0.93 and 0.85) in WT and (0.19, 0.42 and 0.38) in *Cry*-null mice, respectively. There was no significant difference in temporal *Cx43* mRNA levels in *Cry*-null mice by one-way ANOVA. (**g**) Immunoblots

showing temporal changes in protein levels of Cx43 in WT-mouse bladder (three independent samples for each time point). (**h**) Immunostaining of the muscle layer in mouse urinary bladder showing a difference in immunoreactivity with a decrease in Cx43 at CT4 compared to CT16. Representative photographs of three replicated experiments with similar results are shown. Bar, 50 μm. *$P < 0.05$ and **$P < 0.01$ by one-way ANOVA with Tukey's *post hoc* test in **f** and **g**. Error bars represent s.e.m. in **b** and **d**, and s.d. in **e**-**g**. For the relative levels, the maximal values of WT were set as 1 in **e** and **f**. F(x,y), x=DF for the time factor; y=error DF in **b** and **c**.

Figure 3 *Cx43* and clock-gene expression rhythms in rats and their correlation with micturition rhythm. (**a**) Patterns of UVVM in female Sprague-Dawley rats under LD conditions for 2 days (n=15, 1001 micturitions; F(2.7[DF for the time factor],38.3[error DF])=11.9; **P* < 0.005 by one-way repeated measures ANOVA with a Greenhouse-Geisser correction). (**b**) Temporal mRNA accumulation of *Per2 Bmal1* and *Cx43* in the rat bladder under LD and DD conditions (n=5 and n=2 for each time point, respectively). MaxCorrs were 0.87, 0.90 and 0.84 in LD conditions, respectively, and 0.98, 0.95 and 0.93 in DD conditions, respectively. (**c**) Temporal Cx43 protein accumulation in the rat bladder under DD conditions as shown by immunoblotting. (**d**) Immunostaining of Cx43 in the rat bladder under DD conditions (red, Cx43; blue, DAPI). The scale bar indicates 100 μm. Error bars represent s.e.m. in **a** and s.d. in **b**. For the relative expression, maximal values were set as 1 in **b**.

Figure 4 Oscillation of the circadian clock, *Cx43* and gap-junction function in bladder muscle cells without systemic control. (**a**) Oscillation of luminescence in bladder *ex vivo* slice culture obtained from m*Per2*^{Luciferase} knock-in (*Per2::luc*) mice. The period of oscillation was 24.92 ± 0.56 (mean ± s.d.) (n=10). The muscle layer of the bladder is shown by alpha smooth muscle actin (αSMA) immunostaining. m, muscle. The scale bar indicates 100 μm. The oscillation of luminescence is also shown by a movie in Supplementary Movie 1. (**b**) Temporal variation of *Per2*, *Bmal1* and *Cx43* mRNA levels in serum-shocked rat bladder smooth muscle cells (BSMC). **P* < 0.01 against the nadir of each genes' mRNA levels (time 12 for *Per2*, time 48 for *Bmal1* and time 64 for *Cx43*) by one-way ANOVA with Dunnett's *post hoc* test (n=3–6). SS, serum shock. (**c**) Immunoblots showing temporal changes in Cx43 protein levels with αSMA as a loading control in serum-shocked rat BSMC. (**d**) Immunostaining of Cx43 at times 12, 24, 36 and 48 hours in serum-shocked rat BSMC (red, Cx43; blue, DAPI). Arrow heads indicate typical plaques of gap junctions. Representative data of two replicate experiments with similar results in **c** and **d** are shown. (**e**) Oscillation of gap junction function evaluated by Lucifer yellow (LY) microinjection in serum-shocked rat BSMC. One representative photograph at times 12, 24, 36 and 48 hours (green, LY; blue, Hoechst 33342) and overall quantification of the degree of dye-coupling (n=6–9, a

total of 71 injections) are shown. *P < 0.05 and **P < 0.01 vs. time 24 hours by one-way ANOVA with Tukey-Kramer's *post hoc* test. Similar significant differences were obtained in two independent experiments. Error bars represent s.e.m.. Scale bars in **d** and **e** indicate 100 μm. For relative levels, the values before serum shock were set as 1 in **b**.

Figure 5 Rev-erbα upregulates Cx43 expression. (**a**) Dose-dependent activation of *Cx43* transcription by Rev-erbα. Cells used are HEK293T (n=3 for each dose). (**b**) Impaired activation of *Cx43* transcription by a mutant of Rev-erbα without 127–206 amino acids from the N-terminal (Rev-Mut). Cells used were HEK293T (n=3 for each dose). (**c**) Activation of *Cx43* transcription by Rev-erbα in rat BSMC (n=6 for each dose). **P* < 0.01 vs. Rev-erbα (-) by one-way ANOVA with Dunnett's *post hoc* test in **a-c**. Similar data obtained in three independent experiments for **a** and **b,** and in two independent experiments for **c**. (**d**) Suppression of Cx43 expression by knock-down of endogenous Rev-erbα in BSMC. Three types of *Rev-erbα* siRNAs, containing high (si-1), middle (si-2) and low (si-3) GC ratios or their controls containing corresponding GC ratios were transfected. (n=4). Messenger RNA and protein expression (data of si-3) was normalized by 18s ribosomal RNA and GAPDH, respectively. Interference of *Rev-erbα* mRNA significantly decreased mRNA expression of *Cx43* and increased *Bmal1* compared with their corresponding controls (F(1[DF for the treatment factor],18[error DF])=324 for *Rev-erbα*, 9.7 for *Cx43* and 11.7 for *Bmal1*. **P* < 0.01 by two-way ANOVA). Temporal bladder *Rev-erbα* mRNA accumulation in WT and *Cry*-null mice (n=3). (**e**) and in rats under LD (n=5) and DD (n=2) conditions (**f**). **P* < 0.05 vs. CT8 and ***P* < 0.01 vs. CT0, 16 and 20 in WT by one-way ANOVA with

Tukey's *post hoc* test. No significant difference in *Cry*-null mice. MaxCorrs were WT, 0.98; *Cry*-null, 0.31; rats in LD, 0.84; in DD, 0.93. The maximal value of WT was set as 1. Error bars represent s.d. in **a**-**f**. For relative levels, Rev-erbα (-) was set as 1 in **a**-**c**.

Figure 6 Sp1 dependent activation of Cx43 expression by Rev-erbα. (**a**) Sequences including Sp1 sites are indispensable for *Cx43* promoter activation by Rev-erbα. **P* < 0.001 vs. the control of each construct and †*P* < 0.001 vs. -54 (without Sp1 sequences) construct by two-way ANOVA with Bonferroni's *post hoc* test (n=3 for each). (**b-e**) Rev-erbα and Sp1 activate *Cx43* expression using Sp1 sites. (**b**) Diagram of *Cx43* promoter sequences including three Sp1 sites, labelled as Sp1A, B and C. The asterisk indicates corresponding nucleotide sequences among humans, rats and mice. (**c**) Dose dependent activation of *Cx43* transcription by Sp1 and Rev-erbα with Sp1. **P* < 0.001 vs. the value -without Sp1 and Rev-erbα, and †*P* < 0.001 by one-way ANOVA with Tukey's *post hoc* test (n=3 for each). (**d**) Immunoblot analysis of the effect of Sp1 and Rev-erbα on expression of Cx43 and Bmal1 (control of negative regulatory effect by Rev-erbα). (**e**) Impaired activation of pCx43 with the Sp1 sites mutation by Sp1 and Rev-erbα. **P* < 0.001 vs. the controls of each construct, and †*P* < 0.001 vs. the *Mut*C construct by two-way ANOVA with Bonferroni's *post hoc* test (n=3 for each group). Error bars represent s.d. in **a**, **c** and **e**. Cells used were HEK293T in all transfection experiments. The control without Rev-erbα and Sp1 was set as 1 in **a**, **c** and **e**. One representative of two experiments with similar results is shown in **a**, **c**, **d** and **e**.

Figure 7 Rhythmic assembly of Rev-erbα and Sp1 at Sp1 sites of the *Cx43* promoter. (**a**) Co-immunoprecipitation showing a complex formation between HA-tagged Rev-erbα and DDDDK-tagged Sp1 transfected in HEK293T cells, using antibodies for HA and DDDDK. One representative of three experiments with similar results is shown. (**b**) Chromatin immunoprecipitation (ChIP) assay using antibodies for HA and DDDDK in HEK 293T cells transfected with HA-Rev-erbα and DDDDK-Sp1. Analyses by real-time RT-PCR are shown, targeted against endogenous Sp1 sites of the human *Cx43* promoter and its negative control sites, which are approximately 7 kbp up- (5') and 10 kbp down- (3') stream from the transcription start site. A ChIP assay using an antibody for RNA polymerase II and primers for human *GAPDH* promoter was used as a positive control. One representative of two experiments with similar results is shown. (**c**) Temporal *Sp1* mRNA accumulation in the mouse bladder (n=3 for each time point). There were no significant differences among time points by one-way ANOVA. (**d**) Oscillations of *Rev-erbα* mRNA (left) and protein expression (right) in serum-shocked rat BSMC (top row). $*P < 0.01$ vs. the nadir value (time 8) by one-way ANOVA with Dunnett's *post hoc* test (n=3–6). SS, serum shock. The ChIP assay, using an antibody for endogenous Rev-erbα, was analysed by RT-PCR targeted against endogenous Sp1 sites of the rat *Cx43* promoter and negative control sites, which are

approximately 8 kbp up- (5’ negative) and down- (3’ negative) stream (bottom row). *β-actin* is a positive control. Results of real-time RT-PCR are added; it was targeted against Sp1 sites of the *Cx43* promoter, which was immunoprecipitated using an antibody for Rev-erbα (corresponding to the framed bands, bottom). One representative of two experiments with similar results is shown. (**e**) A mechanistic scheme of *Cx43* oscillation, controlled by the Rev-erbα and Sp1 complex binding to Sp1 sites of the *Cx43* promoter. Error bars represent s.d. in **c** and s.e.m. in **d**. For relative levels, the maximal value was set as 1 in **c** and the values before serum shock (time 0) was set as 1 in **d**.

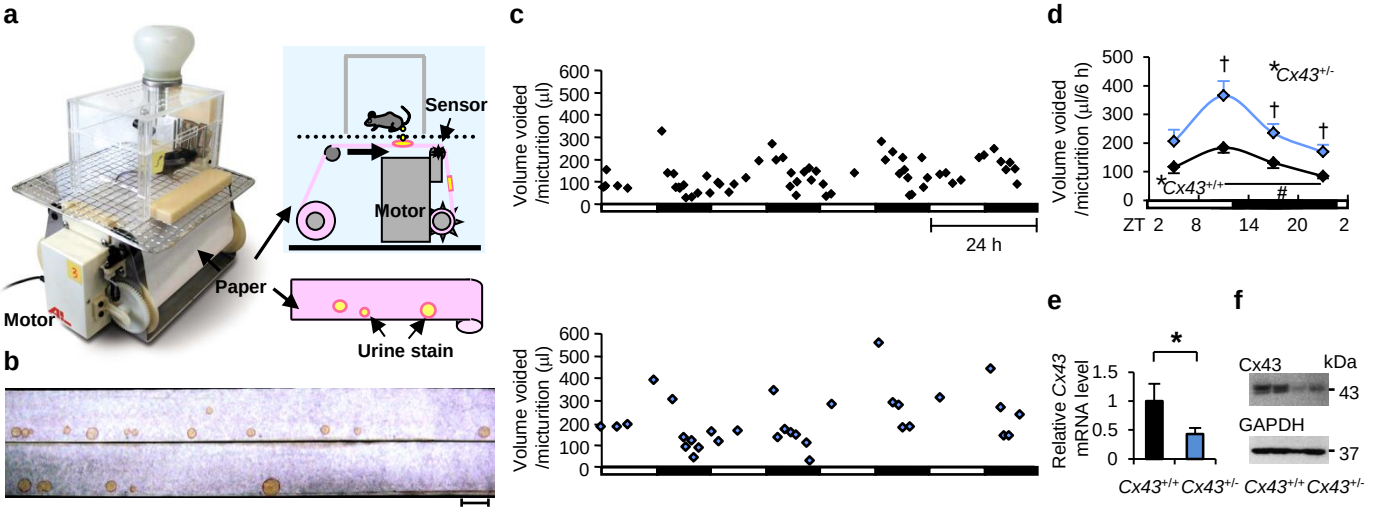
a
Sensor
Motor
Paper
Motor
Urine stain
b
c
Volume voided /micturition (μl)
600
500
400
300
200
100
0
24 h
Volume voided /micturition (μl)
d
Volume voided /micturition (μl/6 h)
500
400
300
200
100
0
*Cx43+/-
*Cx43+/+
#
ZT 2 8 14 20 2
e
Relative Cx43 mRNA level
1.5
1
0.5
0
*
Cx43+/+ Cx43+/- Cx43+/+ Cx43+/-
f
Cx43
kDa
43
GAPDH
37

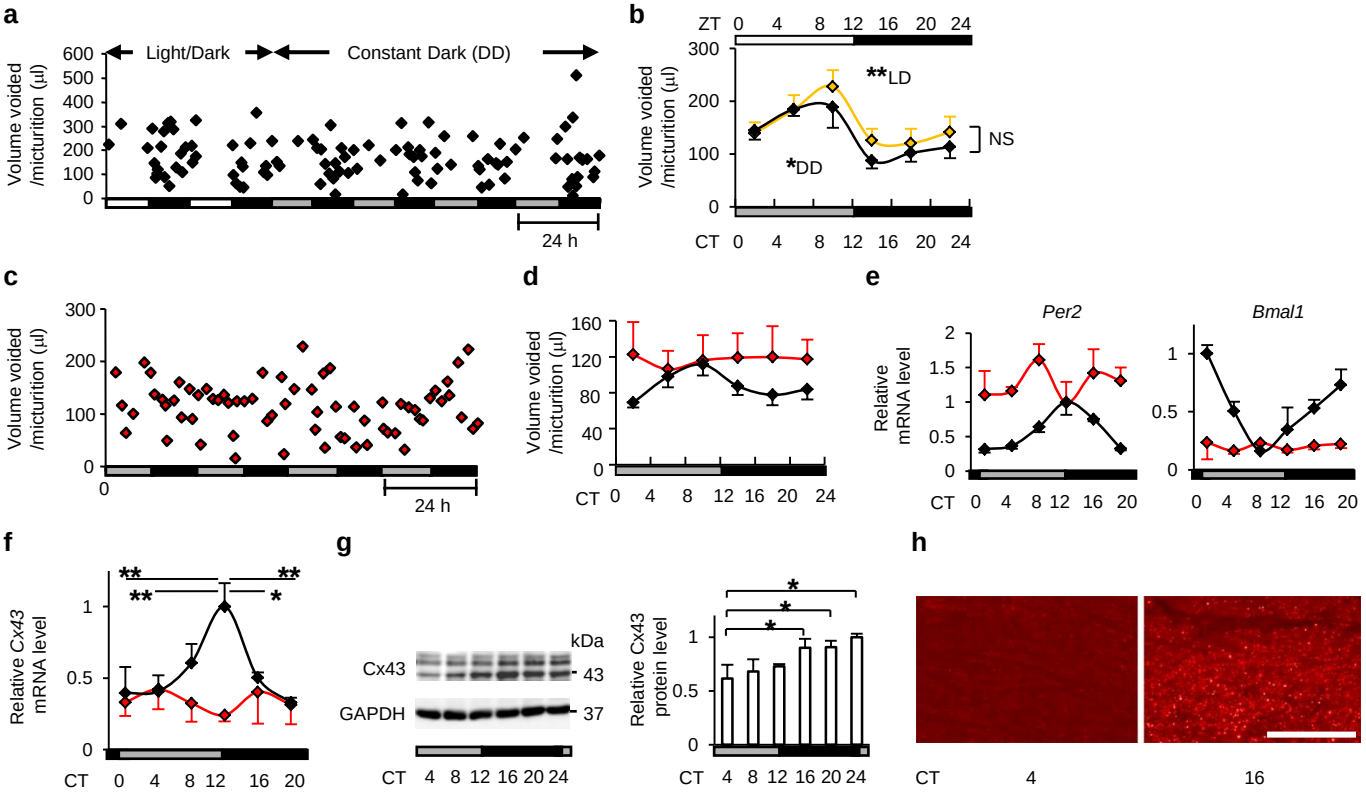
a
Light/Dark
Constant Dark (DD)
Volume voided /micturition (μl)
600
500
400
300
200
100
0
24 h
b
ZT 0 4 8 12 16 20 24
Volume voided /micturition (μl)
300
200
100
0
**LD
*DD
NS
CT 0 4 8 12 16 20 24
c
Volume voided /micturition (μl)
300
200
100
0
0
24 h
d
Volume voided /micturition (μl)
160
120
80
40
0
CT 0 4 8 12 16 20 24
e
Per2
Bmal1
Relative mRNA level
2
1.5
1
0.5
0
CT 0 4 8 12 16 20
0 4 8 12 16 20
f
Relative Cx43 mRNA level
**
**
**
*
1
0.5
0
CT 0 4 8 12 16 20
g
kDa
Cx43
43
GAPDH
37
CT 4 8 12 16 20 24
Relative Cx43 protein level
*
*
*
1
0.5
0
CT 4 8 12 16 20 24
h
CT 4 16

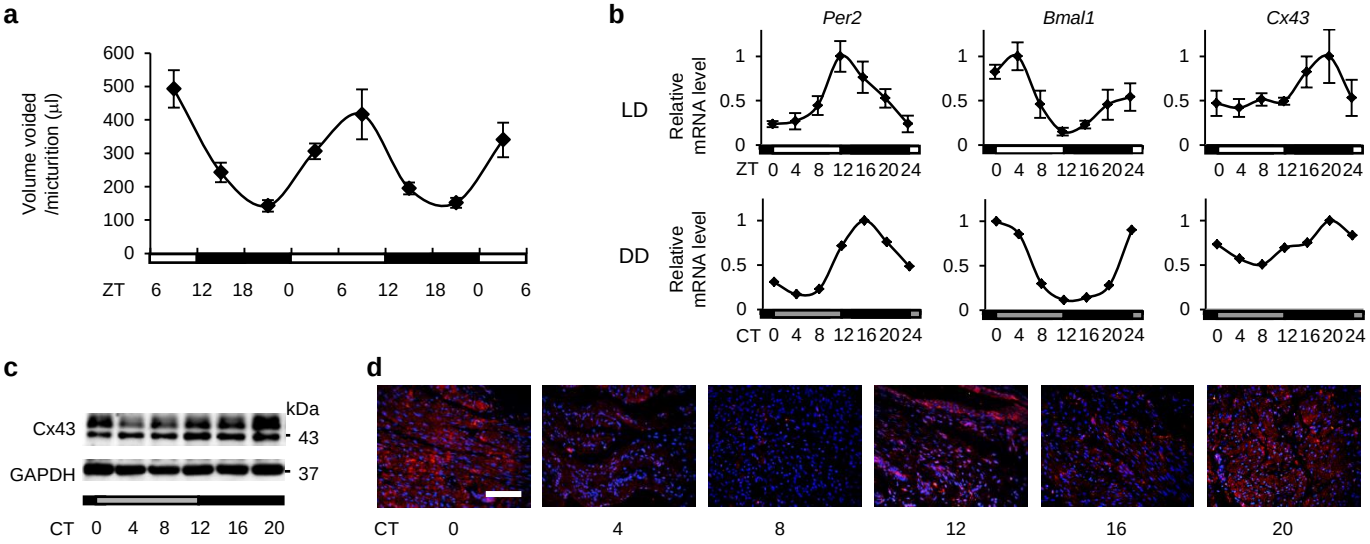
a
Volume voided /micturition (μl)
600
500
400
300
200
100
0
ZT 6 12 18 0 6 12 18 0 6
b
Per2
Bmal1
Cx43
LD
DD
Relative mRNA level
1
0.5
0
ZT 0 4 8 12 16 20 24
CT 0 4 8 12 16 20 24
c
kDa
Cx43
43
GAPDH
37
CT 0 4 8 12 16 20
d
CT 0 4 8 12 16 20

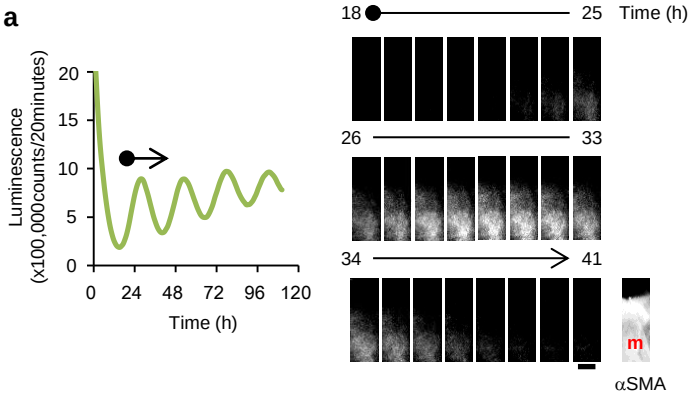
a
18
25
Time (h)
26
33
34
41
m
αSMA
Luminescence
(x100,000counts/20minutes)
Time (h)

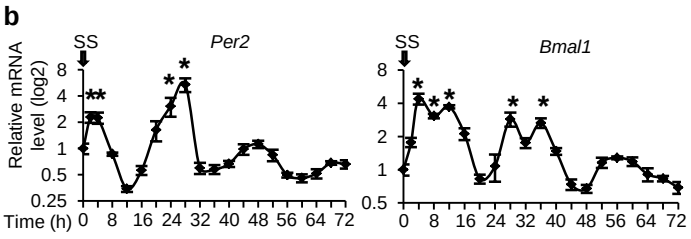
b
SS
Per2
Bmal1
Relative mRNA
level (log2)
Time (h)

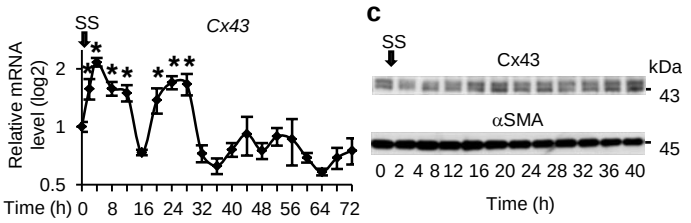
SS
Cx43
Relative mRNA
level (log2)
Time (h)
c
SS
Cx43
kDa
43
αSMA
45
Time (h)

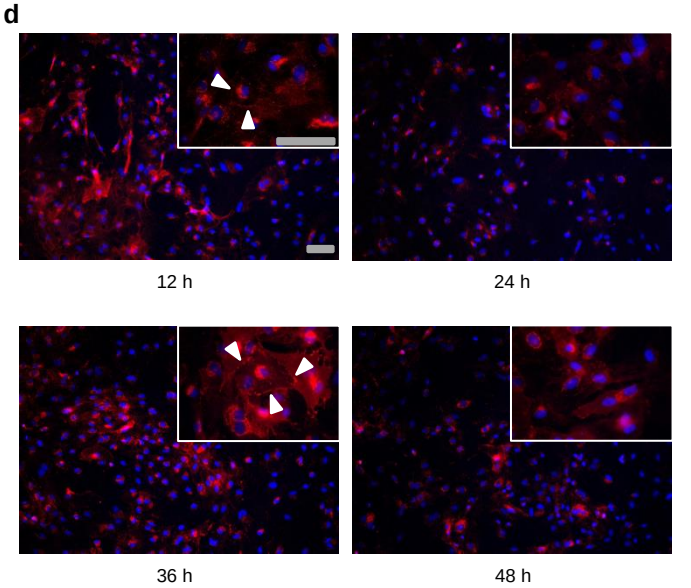
d
12 h
24 h
36 h
48 h

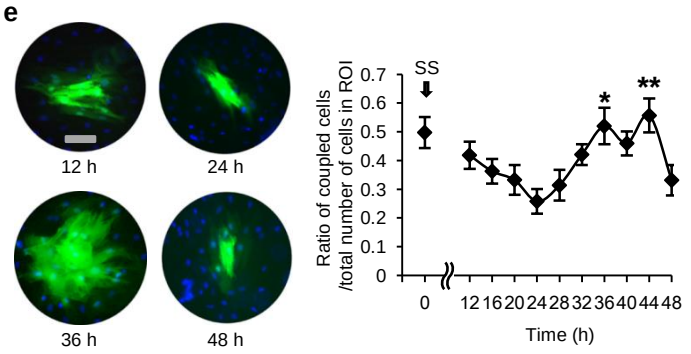
e
12 h
24 h
36 h
48 h
SS
Ratio of coupled cells
/total number of cells in ROI
Time (h)

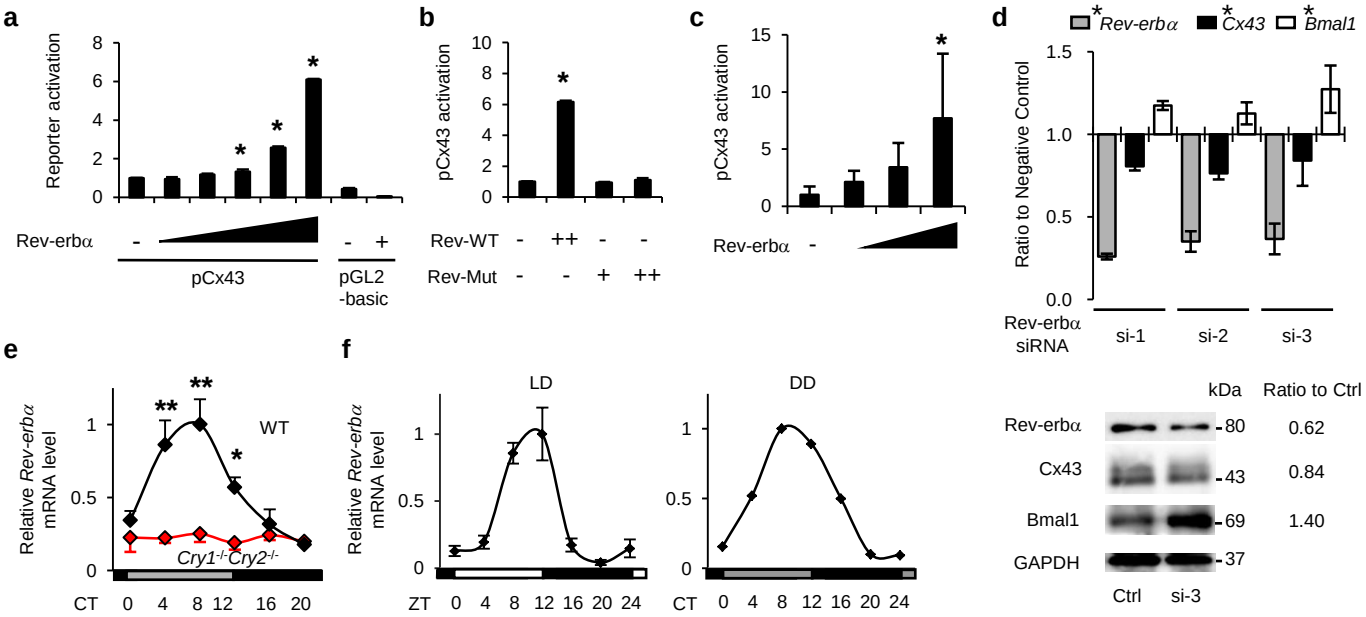
a
Reporter activation
Rev-erbα
pCx43
pGL2
-basic
b
pCx43 activation
Rev-WT
Rev-Mut
c
pCx43 activation
Rev-erbα
d
Rev-erbα
Cx43
Bmal1
Ratio to Negative Control
Rev-erbα siRNA
si-1
si-2
si-3
kDa
Ratio to Ctrl
Rev-erbα
Cx43
Bmal1
GAPDH
80
43
69
37
0.62
0.84
1.40
Ctrl
si-3
e
Relative Rev-erbα mRNA level
WT
Cry1-/-Cry2-/-
CT
f
LD
DD
ZT
CT

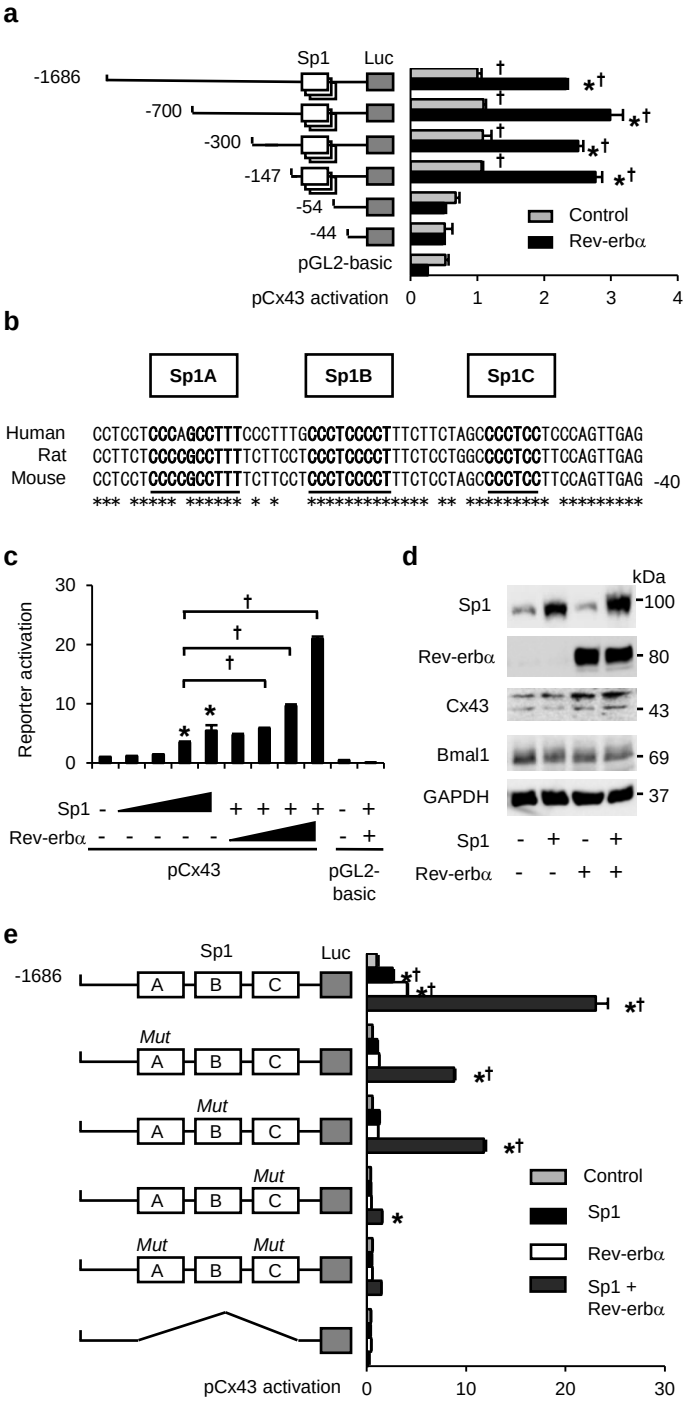
a
Sp1
Luc
-1686
-700
-300
-147
-54
-44
pGL2-basic
Control
Rev-erbα
pCx43 activation
0
1
2
3
4
b
Sp1A
Sp1B
Sp1C
Human CCTCCTCCCAGCCTTTCCCTTTGCCCTCCCCTTTCTTCTAGCCCCTCCTCCCAGTTGAG
Rat CCTTCTCCCCGCCTTTTCTTCCTCCCTCCCCTTTCTCCTGGCCCCTCCTTCCAGTTGAG
Mouse CCTCCTCCCCGCCTTTTCTTCCTCCCTCCCCTTTCTCCTAGCCCCTCCTTCCAGTTGAG -40
c
Reporter activation
30
20
10
0
Sp1
Rev-erbα
pCx43
pGL2-basic
d
kDa
Sp1
Rev-erbα
Cx43
Bmal1
GAPDH
100
80
43
69
37
e
Sp1
Luc
-1686
A
B
C
Mut
Control
Sp1
Rev-erbα
Sp1 +
Rev-erbα
pCx43 activation
0
10
20
30

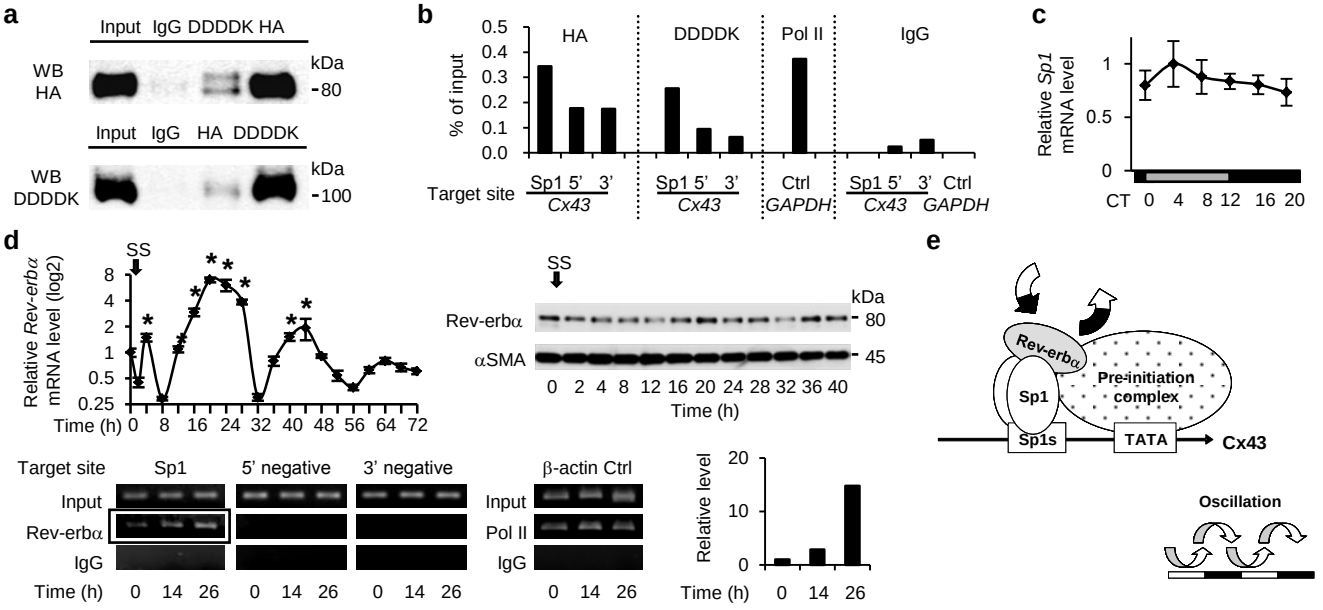
a
Input IgG DDDDK HA
WB HA
kDa
80
Input IgG HA DDDDK
WB DDDDK
kDa
100
b
% of input
HA
DDDDK
Pol II
IgG
Target site
Sp1 5' 3'
Cx43
Ctrl
GAPDH
c
Relative Sp1 mRNA level
CT 0 4 8 12 16 20
d
Relative Rev-erbα mRNA level (log2)
SS
Time (h) 0 8 16 24 32 40 48 56 64 72
Rev-erbα
αSMA
kDa
80
45
0 2 4 8 12 16 20 24 28 32 36 40
Target site
Sp1
5' negative
3' negative
β-actin Ctrl
Input
Rev-erbα
IgG
Pol II
Relative level
Time (h) 0 14 26
e
Rev-erbα
Sp1
Pre-initiation complex
Sp1s
TATA
Cx43
Oscillation

Supplementary Information for

Involvement of urinary bladder Connexin43 and the circadian clock in coordination of diurnal micturition rhythm

Hiromitsu Negoro,[1,2] Akihiro Kanematsu,[1,3] Masao Doi,[4] Sylvia O. Suadicani,[5,6] Masahiro Matsuo,[4] Masaaki Imamura,[1] Takeshi Okinami,[1] Nobuyuki Nishikawa,[1] Tomonori Oura,[7] Shigeyuki Matsui,[8] Kazuyuki Seo,[4] Motomi Tainaka,[4] Shoichi Urabe,[4] Emi Kiyokage,[9] Takeshi Todo,[10] Hitoshi Okamura,[4]* Yasuhiko Tabata,[2] and Osamu Ogawa[1]*

Correspondence should be addressed to
H.O (E-mail: okamurah@pharm.kyoto-u.ac.jp)
or
O.O (E-mail: ogawao@kuhp.kyoto-u.ac.jp).

Supplementary Information includes:

Supplementary Figure S1

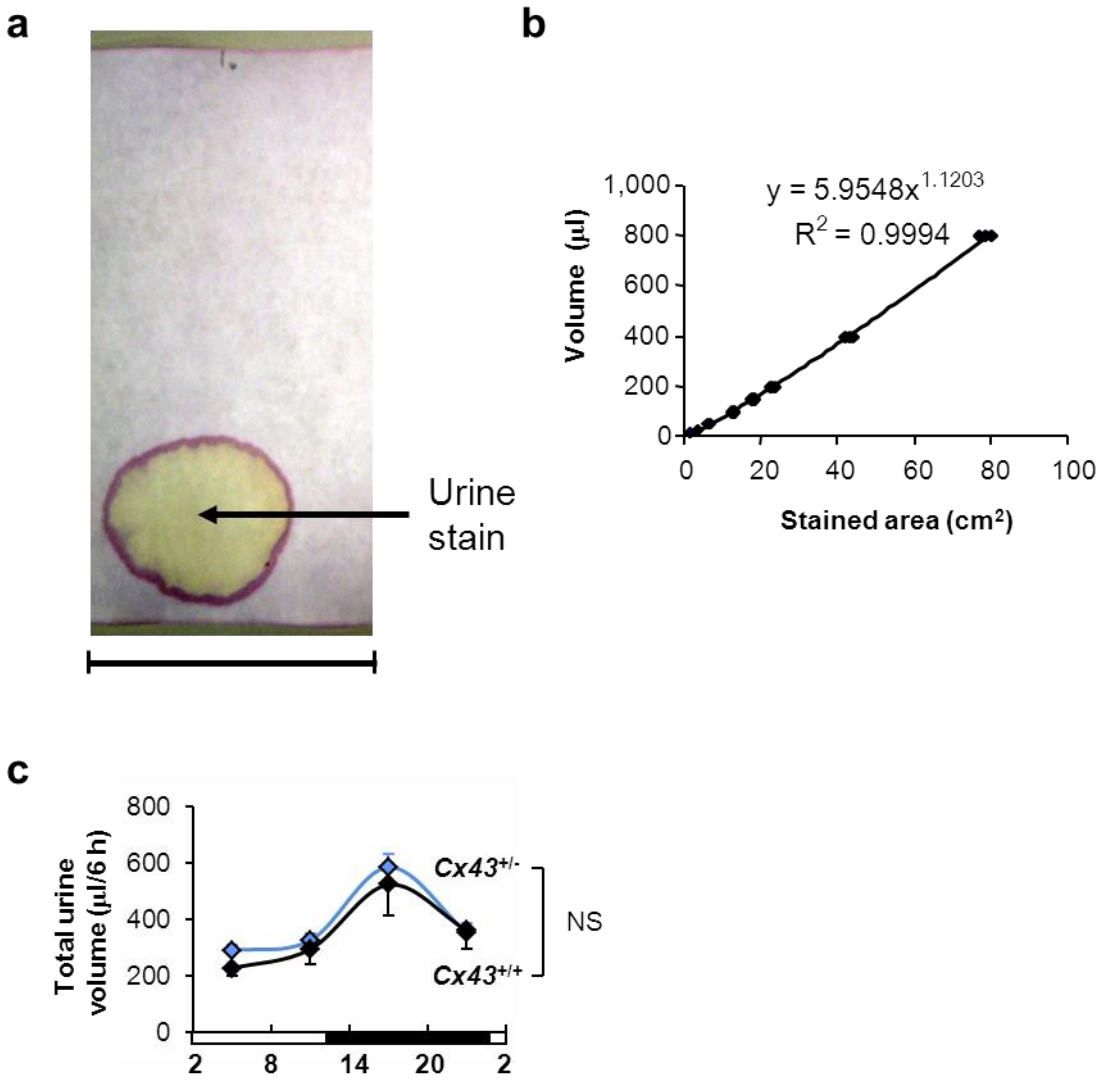

Supplementary Figure S1 | Automated Voided Stain on Paper (aVSOP) method and characteristics of *Cx43*$^{+/+}$ and *Cx43*$^{+/-}$ mice. (**a**) A representative urine stain with a deep purple edge. The scale bar indicates 10 cm, corresponding to 1 hour. (**b**) A standard curve was constructed from 10 to 800 µl of normal saline and their corresponding stained areas (n=3 for each volume). (**c**) There were no significant differences in total urine volume per 6 hours among *Cx43*$^{+/+}$ and *Cx43*$^{+/-}$ mice (two-way repeated measures ANOVA, n=4 for each mice). No marked difference was observed in body weights (23.4 ± 3.5 g in *Cx43*$^{+/+}$ mice and 22.9 ± 3.0 g in *Cx43*$^{+/-}$ mice, mean ± s.d., n=4 for each mice).

Supplementary Figure S2

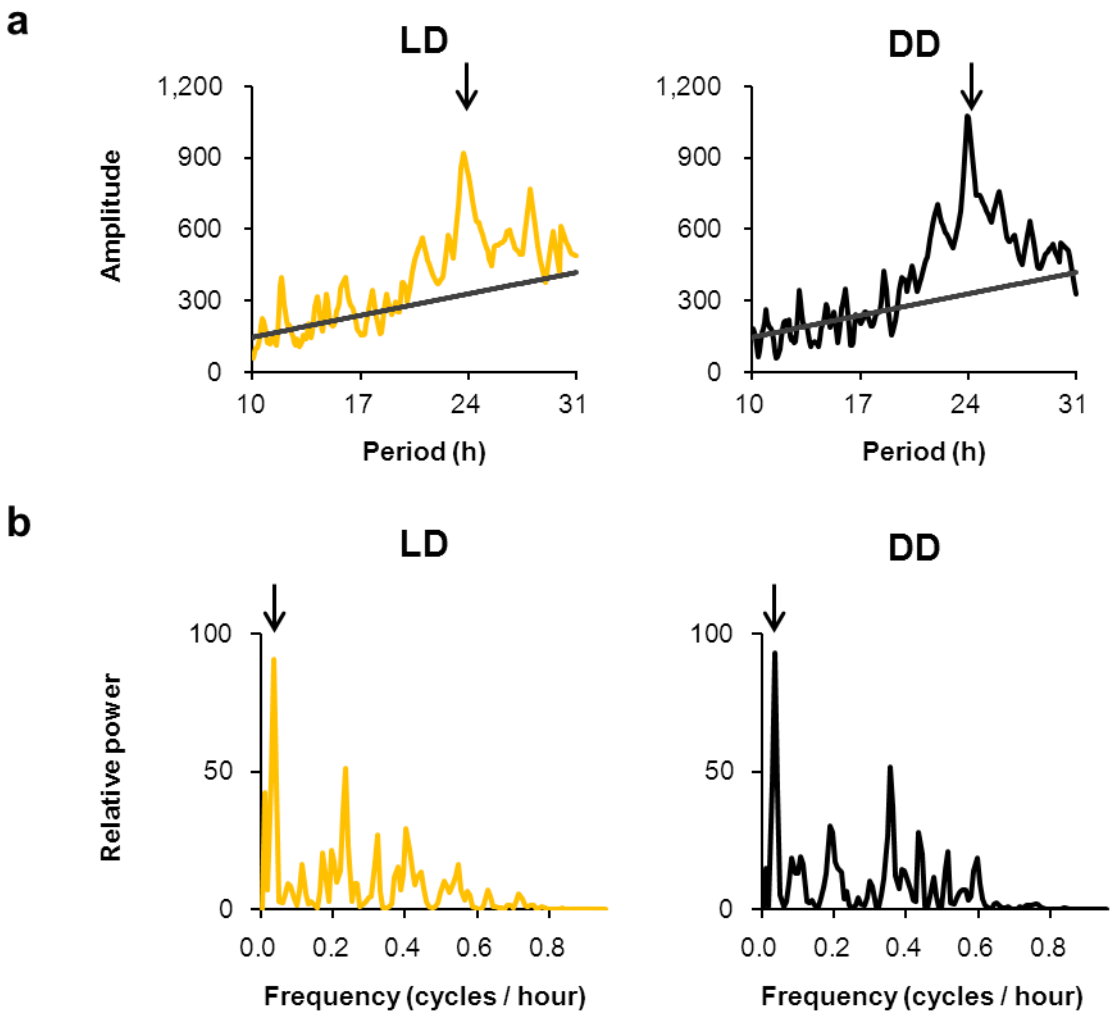

Supplementary Figure S2 | Analyses of diurnal rhythm in UVVM under LD and DD conditions. (**a**) Representative χ^2 periodograms of UVVM under LD (left) and DD (right) conditions show a peak at 24 hours, indicated by arrow heads. (**b**) Circadian amplitudes in **a** were quantified as relative power calculated by Fourier transform (0.042 cycles per hour, indicated by arrow heads). Relative power spectral densities to 24 hours (rPSD) of five mice in LD and DD were 0.060 ± 0.026 and 0.053 ± 0.013, respectively (mean ± s.e.m.), with no significant difference by Mann-Whitney *U*-test.

Supplementary Figure S3

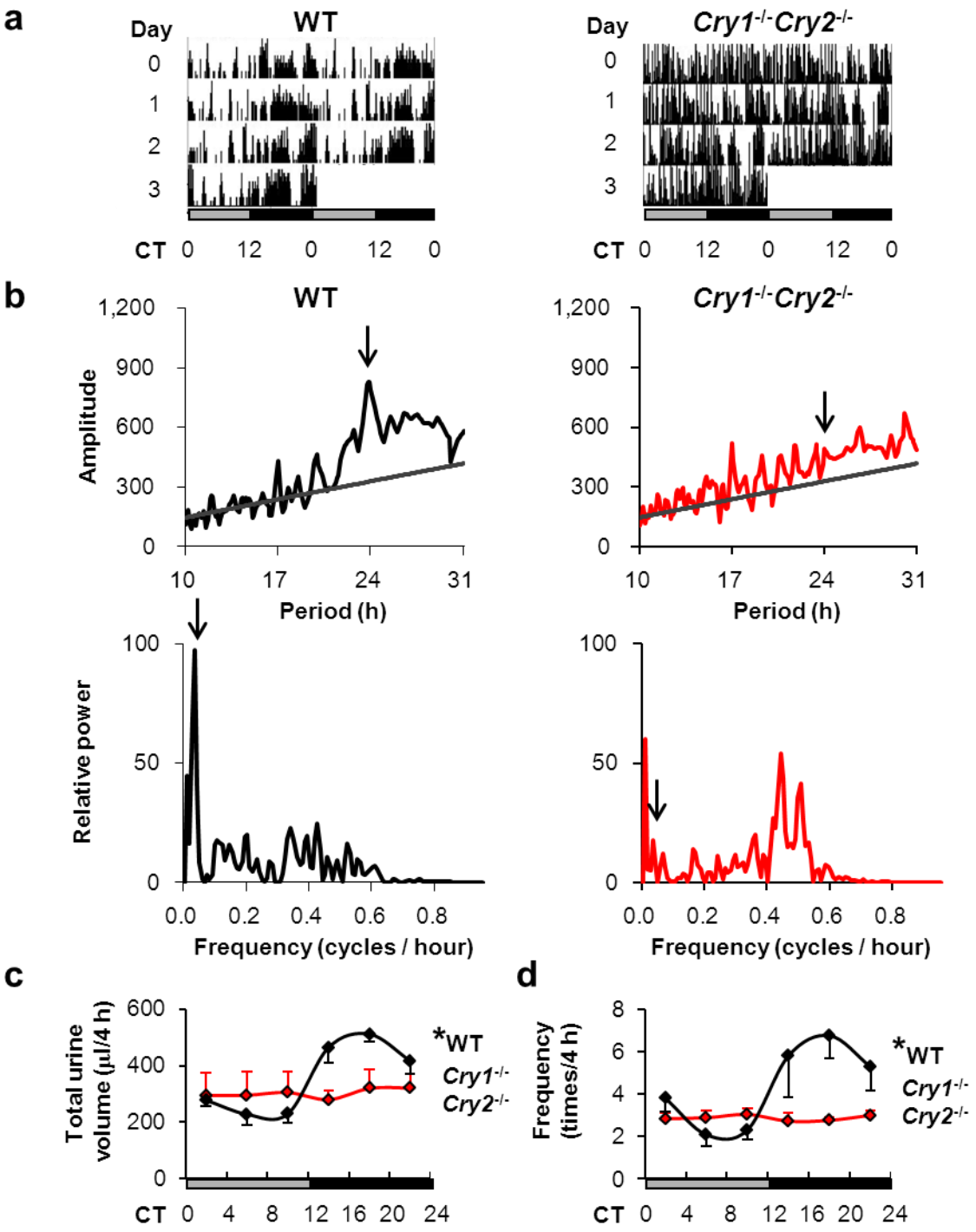

Supplementary Figure S3 | *Cry*-null mice have disturbed rhythmicity in locomotor activity and micturition behaviour. (**a**) Actograms of WT and *Cry*-null mice. Each following day was double-plotted. (**b**) One representative χ^2 periodogram and circadian amplitude of UVVM in WT and *Cry*-null mice. Circadian periodicity (indicated by arrow heads) shown in the WT mice was disturbed in *Cry*-null mice. Circadian rhythmicity, demonstrated by rPSD, in *Cry*-null mice was significantly lower than that in WT mice (0.009 ± 0.002 vs. 0.039 ± 0.015 [mean ± s.e.m.], $P < 0.05$ by Mann-Whitney *U*-test; n=5 for each model). (**c**) Significant temporal changes in total urine volume per 4 hours observed in WT mice ($F(5,20)=9.8$, $^*P < 0.005$ by one-way repeated measures ANOVA) were not observed in *Cry*-null mice, and rPSD in *Cry*-null mice was significantly lower than that in WT mice (0.035 ± 0.013 vs. 0.135 ± 0.027, $P < 0.05$ by Mann-Whitney *U*-test, n=5 for each model). (**d**) Significant temporal changes in urinary frequency per 4 hours in WT mice ($F(5,20)=14.0$, $^*P < 0.005$ by one-way repeated measures ANOVA) were not observed in *Cry*-null mice, and rPSD in *Cry*-null mice was significantly lower than that in WT mice (0.004 ± 0.002 vs. 0.115 ± 0.025, $P < 0.005$ by Mann-Whitney *U*-test, n=5 for each model). Error bars represent s.e.m.. F(x,y), x=DF for the time factor; y=error DF in **c** and **d**.

Supplementary Figure S4

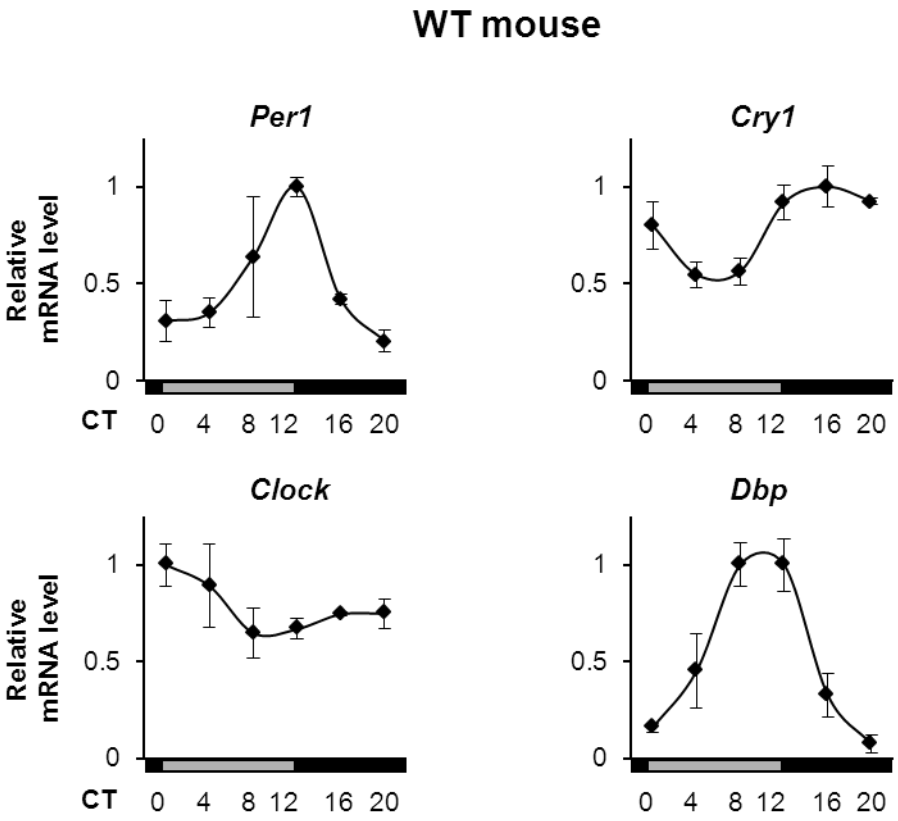

Supplementary Figure S4 | Clock gene expression rhythms of the urinary bladder in WT mice. Temporal mRNA accumulation of *Per1*, *Cry1*, *Clock* and *Dbp* in WT mouse bladder under DD conditions by real-time RT-PCR (n=3 for each time point). MaxCorrs of *Per1*, *Cry1*, *Clock* and *Dbp* were 0.89, 0.96, 0.86 and 0.98, respectively. Error bars represent s.d.. For the relative expression, maximal values were set as 1.

Supplementary Figure S5

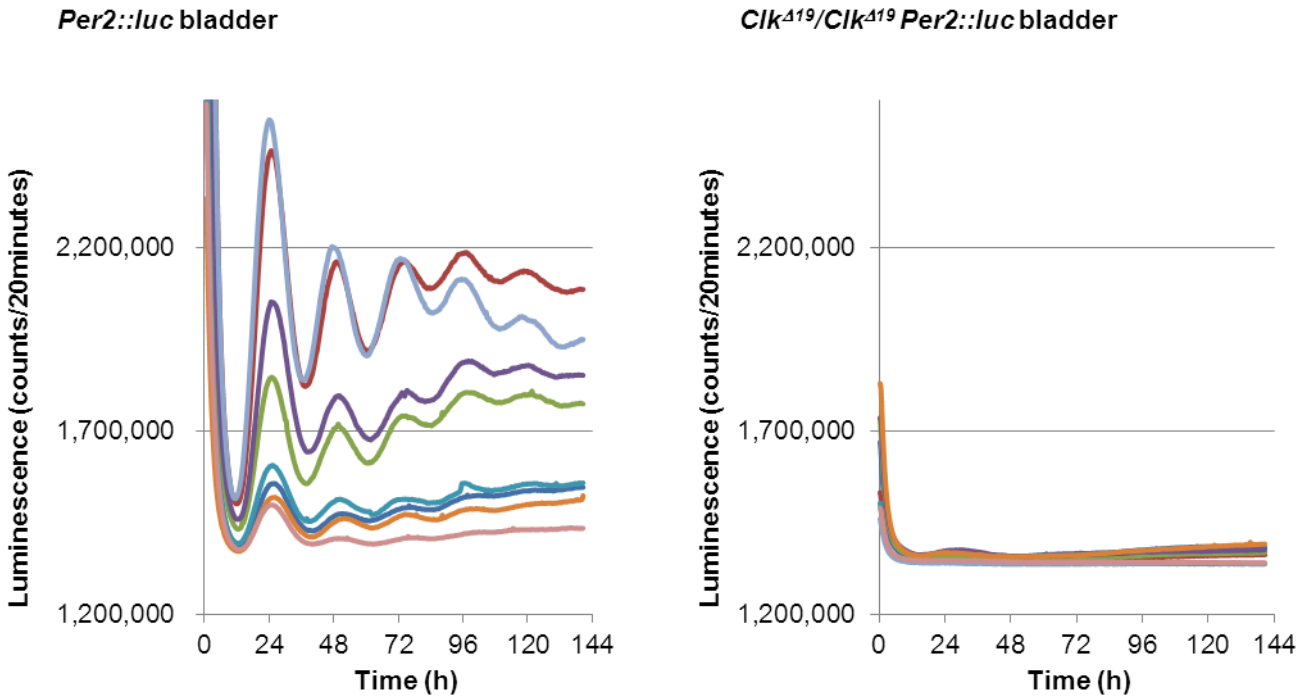

Supplementary Figure S5 | Disturbed oscillations of bladder internal clock in *Clock* mutant *Per2::luc* mice. Oscillations of luminescence observed in bladder *ex vivo* slice culture obtained from m*Per2*^{Luciferase} knock-in (*Per2::luc*) mice (left, n=8), and *Per2::luc* mice with the *Clock*-mutation (*Clk*$^{\Delta 19}$/*Clk*$^{\Delta 19}$)[61] (right, n=8). Note the bioluminescence of each bladder from *Clk*$^{\Delta 19}$/*Clk*$^{\Delta 19}$ mutant *Per2::luc* mice lacked a circadian rhythm.

Supplementary Figure S6

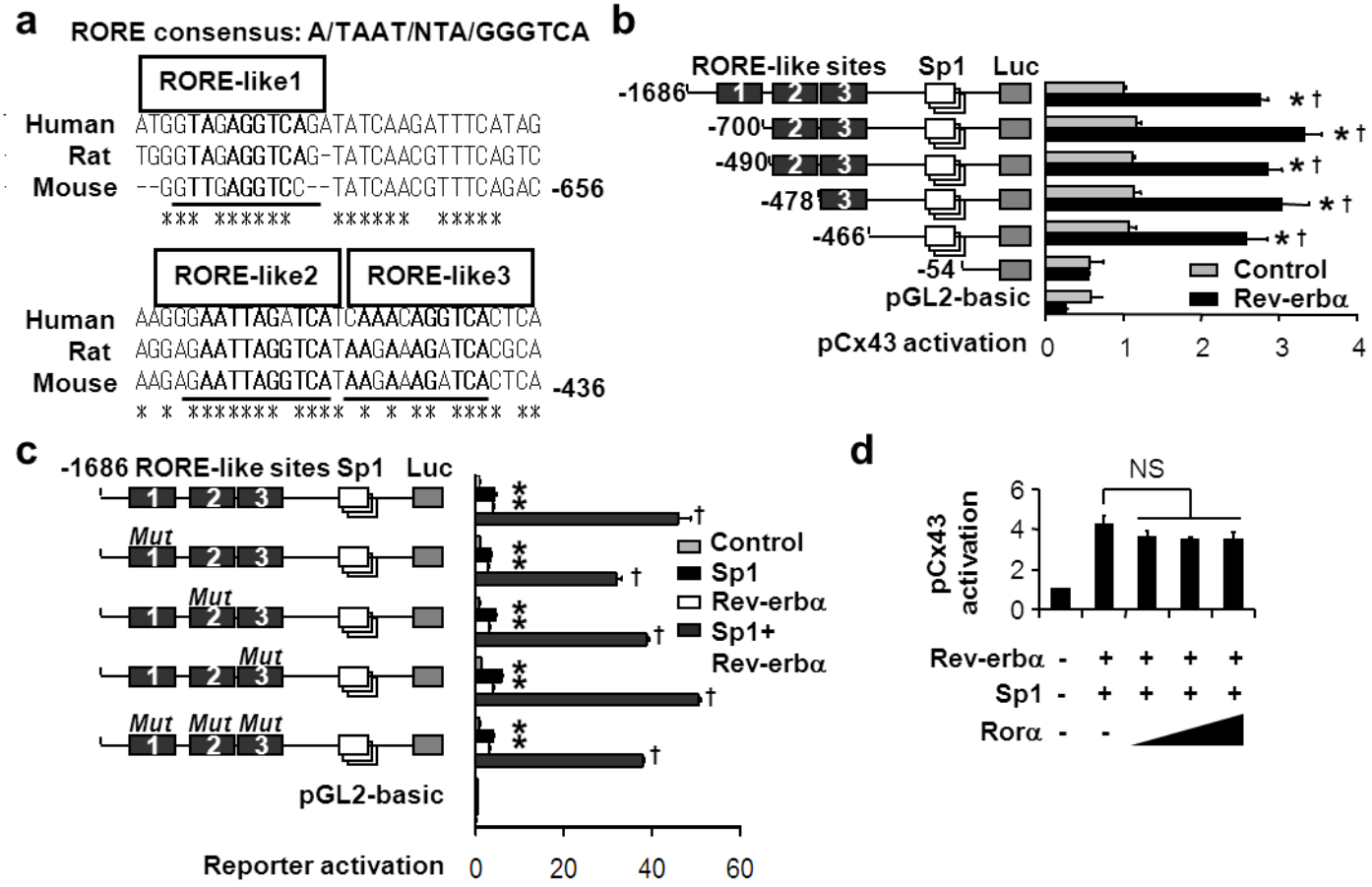

Supplementary Figure S6 | RORE-like site-independent activation of *Cx43* transcription by Rev-erbα. (**a**) Schematic representation of *Cx43* promoter sequences including three RORE-like sites, numbered from the distal to proximal side as RORE-like 1, 2 and 3. The asterisk indicates corresponding nucleotide sequences among humans, rats and mice. (**b**) RORE-like sites are dispensable for *Cx43* promoter activation by Rev-erbα. Truncated mutants of pCx43-luc were transfected with and without Rev-erbα (n=3 for each). **P* < 0.001 vs. the control of each construct and †*P* < 0.001 vs. the -54 (without Sp1 sequences) construct by two-way ANOVA with Bonferroni's *post hoc* test. One representative of two experiments with similar results is shown. (**c**) No effect of mutations in the three predictable RORE-like sites (RORE-like 1, A**GG**TCC→A**CA**TCC; RORE-like 2, A**GG**TCA→A**CA**TCA; and RORE-like 3, A**G**ATCA→A**C**ATCA) on activation by Rev-erbα and Sp1 was observed. **P* < 0.001 vs. the control of each construct and †*P* < 0.001 vs. the control, Sp1 or Rev-erbα of each construct by two-way ANOVA with Bonferroni's *post hoc* test, n=3 for each group. One representative of three experiments with similar results is shown. (**d**) No significant competition by Rorα against Rev-erbα (one-way ANOVA, n=3 for each group). One representative of three experiments with similar results is shown. Error bars represent s.d.. Cells used were HEK293T in all transfection experiments. Similar results were obtained using the same expression vector without coding Rev-erbα or RORα. Five nanogram of pTK-RL was used in **b**-**d** as a transfection efficiency control. For relative expression, Rev-erbα (-) was set as 1 in **b**, Sp1 (-) Rev-erbα (-) in **c** and Rev-erbα (-) Rorα (-) Sp1 (-) in **d**.

Supplementary Discussion The RORE-like sites of the *Cx43* promoter are atypical (**Supplementary Fig. S6a**) because correspondence of RORE-like 1 to the RORE consensus is weak and the base pair number between tandem repeats of RORE-like 2 and 3 is not matched to the reported RORE site bound as a dimer of Rev-erbα[62]. However, the involvement of these RORE-like sites for activation of *Cx43* by Rev-erbα should have been tested, because the activation mechanism by Rev-erbα was contradictory to conventional notion. The truncation mutants of the *Cx43* promoter, whose truncated sites are more specific to the RORE-like sites, did not affect *Cx43* promoter activation (**Supplementary Fig. S6b**). Mutations of RORE-sites also had no effect on activation of the *Cx43* promoter by Rev-erbα, even with Sp1 (**Supplementary Fig. S6c**), which activates the *Cx43* promoter in association with Rev-erbα, as we will demonstrate later in **Fig. 6**. RORα, known as a positive competitor of Rev-erbα at the RORE site of the promoter, did not compete with Rev-erbα/Sp1 for the activation of *Cx43* (**Supplementary Fig. S6d**). In conclusion, RORE-like sites are dispensable for *Cx43* promoter activation by Rev-erbα/Sp1.

Supplementary Figure S7

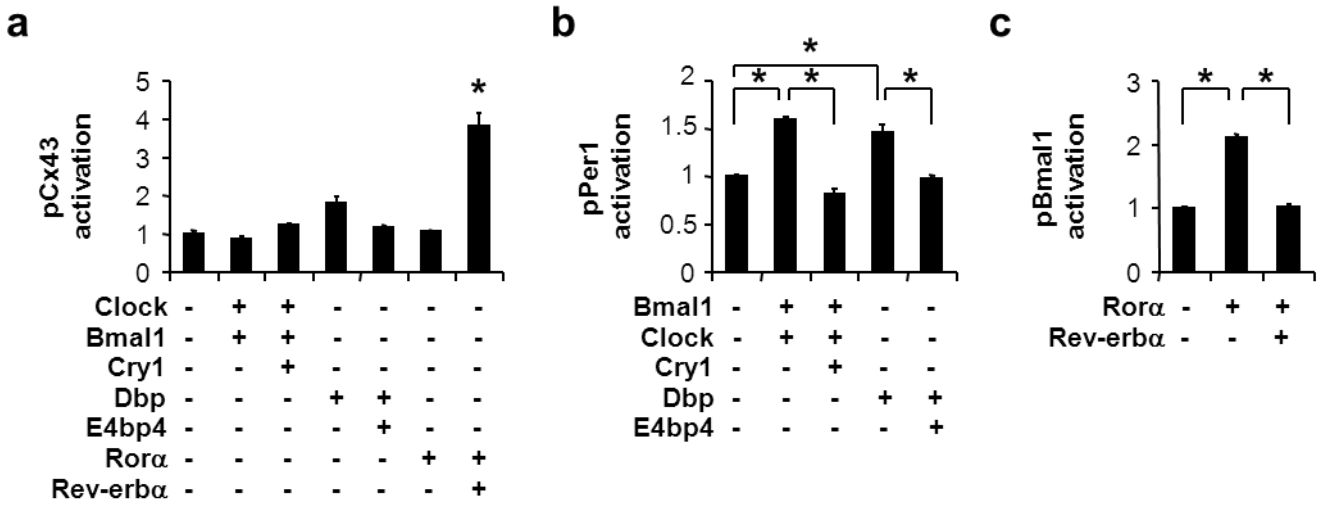

Supplementary Figure S7 | Screening of clock genes for effect on pCx43-luc singled out *Rev-erbα*. (**a**) Rev-erbα had a prominent effect on *Cx43* transcription among clock genes. **P* < 0.0001 vs. controls with no clock gene transfection by one-way ANOVA with Dunnett's *post hoc* test, n=3 for each group. (**b**) Activation of the *Per1* promoter-reporter (pPer1), containing both E-box and D-box elements, by Clock/Bmal1 and Dbp are blocked by Cry1 and E4bp4, respectively. Clock/Bmal1and Cry1 are positive and negative regulators of genes with E-box elements, respectively. Dbp and E4bp4 are positive and negative regulators of genes with D-box elements, respectively. **P* < 0.0001 by one-way ANOVA with Tukey's *post hoc* test, n=3 for each group. (**c**) Activation of the *Bmal1* promoter-reporter (pBmal1), containing RORE sites, by Rorα is blocked by Rev-erbα. **P* < 0.0001 by one-way ANOVA with Tukey's *post hoc* test, n=3 for each group. One representative of three experiments with similar results is shown in **a**-**c**. Error bars represent s.d. in **a**-**c**. The dosage of pPer1-luc and pBmal1-luc was 10 ng; cells used were HEK293T. Controls without clock-gene expression vectors were set as 1**.**

Supplementary Figure S8

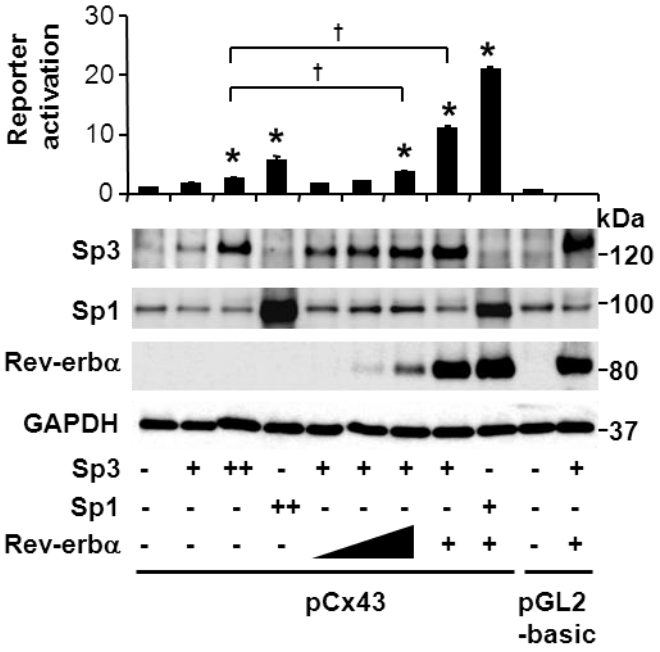

Supplementary Figure S8 | Sp3 is an activator of *Cx43* transcription. The Cx43 transcription was dose-dependently activated by Sp3 and Rev-erbα in HEK 293T cells (n=3 for each group). **P* < 0.05 vs. controls without Sp1, Sp3 and Rev-erbα, and †*P* < 0.005 by one-way ANOVA with Tukey's *post hoc* test. One representative of two experiments with similar results is shown. Immunoblotting shows expression of Sp3, Sp1 and Rev-erbα. Error bars represent s.d.. The relative expression of Sp3 (-) Sp1 (-) Rev-erbα (-) was set as 1.

Supplementary Figure S9

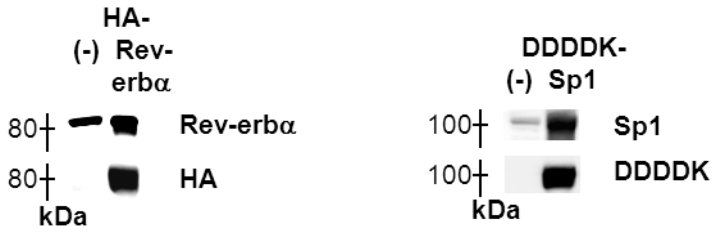

Supplementary Figure S9 | Protein expressions of HA-tagged Rev-erbα and DDDDK-tagged Sp1 expression vectors. Antibodies for Rev-erbα and HA or Sp1 and DDDDK detect proteins of HEK293T cells transfected with expression vectors of HA-tagged Rev-erbα or DDDDK-tagged Sp1, respectively.

Supplementary Table S1

Primers for real-time RT-PCR and ChIP assay

Species	Gene name	Forward (5'→3')	Reverse (5'→3')	Amplicon size (b.p.)
		Primers for real-time RT-PCR		
Mouse	*Cx43* (NM_010288)	CCATCCAAAGACTGCGGAT	GTAATTGCGGCAGGAGGAA	138
	Per1 (NM_011065)	CACTTCGAAACCAGGACACCT	AAACACATCCCGTTTGCAAC	110
	Per2 (NM_011066)	CACACTTGCCTCCGAAATAACTC	AGCGCACGGCTGTCTGA	79
	Cry1 (NM_007771)	GGCGATTTTTGCTTCAGTGTC	CCATTCCTTGAAAAGCCTGG	119
	Clock (NM_007715)	TCAGCAGTCAGTCCATAAACTCC	AAACTGTGACATGCCTTGTGG	104
	Bmal1 (NM_007489)	CCAAGAAAGTATGGACACAGACAAA	GCATTCTTGATCCTTCCTTGGT	80
	Dbp (NM_016974)	GAGACTTTTGACCCTCGGAGAC	TCATCCTTCTGTTCCTCAGGC	107
	Rev-erb α (NM_145434)	ACAGCAGCCGAGTGTCCC	ACACAGTAGCACCATGCCATTC	70
	Sp1 (NM_013672)	ACCATGAGCGACCAAGATCA	CCCATTATTGCCACCAACATC	81
Rat	*Cx43* (NM_012567)	CATTAAGTGAAAGAGAGGTGCCC	GCAGCCAGGTTGTTGAGTGT	210
	Per2 (NM_031678)	GATCTGATCGAGACCCCTGTG	GAATAATCGAAAGGCTGCCC	110
	Bmal1 (NM_024362)	TCGGCGCTCTTTCTTCTGTAG	ACCCGTATTTCCCCGTTCA	276
	Rev-erb α (NM_145775)	AAGCTTAACGGCATGGTGCTACTG	TGGATGTTCTGCTGGATGCTCC	125
	Sp1 (NM_012655)	ACCATGAGCGACCAAGATCA	CCCGTTATTGCCACCAACA	78
		Primers for ChIP assay		
Human	Sp1 site of *Cx43* (NM_000165)	TCCTCCCAGCCTTTCCCTT	AAAAGCTTTTTTGTAACTTGGAGCA	136
	Upstream sequence (5'neg)(-7027/-6922)	AACTTGACTGACCGCAGGG	GGCTTGACGTGTTTGGAAGA	106
	Downstream sequence (3'neg)(11770/11862)	AAGAGATCCCTGCCCACATC	ACCAAGGACACCACCAGCA	93
Rat	Sp1site of *Cx43* (NM_012567)	CTTCTCCCCGCCTTTTCTT	TCTAACTTGGAGCGCAGAGCT	101
	Upstream sequence (5'neg)(-8089/-7965)	TGCTCACTGTTCCATCAGAGAA	AGGCCACAAATGGAAGCTG	125
	Downstream sequence (3'neg)(8354/8461)	CCTTGTTGGACTGGAACATTGT	GTGGAAGCTCGTGCCTATAGTTTA	108

Cx43, *Connexin43*

Supplementary Table S1 | Primers for real-time RT-PCR and chromatin immunoprecipitation (ChIP) assay. Primers were designed using Primer Express 2.0 software (Applied Biosystems) or according to previous reports[63,64].

Supplementary Methods.

Microarray analysis of the mouse bladder. Whole bladder RNA of female C57BL/6 mice sacrificed at CT 0, 4, 8, 12, 16 and 20 as described above was used (n=2 for each time point). A total of 250 ng of qualified RNA was employed for the synthesis of Cy3 labelled cRNA, which was qualified and hybridized to the Whole Mouse Genome Oligo Microarray (44K; Agilent Technologies) according to the manufacturer's protocol (entrusted to DNA Chip Research, Inc., Yokohama, Japan). Statistical analysis of microarray data was performed using R statistical software (version 2.8.1, 2008-12-22) with BioConductor (version 2.3). Signal processing was performed by Agilent Feature Extraction (version. 9.5.3). Normalization was performed based on the Agi4x44PreProcess package (version 1.2.0). The mgug4122a.db package (version 2.2.5) was used for annotation of each probe. Selection of circadian-oscillated genes was based on the modified procedure of Yamada *et al*[35] and McDonald *et al*[34]. Specifically, we calculated correlation coefficients between each six-point time course and 60 different-phased cosine curves with six time points. For each probe, we selected one cosine curve with MaxCorr from the 60 different-phased cosine curves. The false-positive proportion was estimated on the basis of the null distribution of maximum correlations derived from randomly generated expression profiles.

Supplementary References.

61. King DP et al. Positional cloning of the mouse circadian clock gene. *Cell* **89,** 641-653 (1997).
62. Harding HP & Lazar MA. The monomer-binding orphan receptor Rev-Erb represses transcription as a dimer on a novel direct repeat. *Mol Cell Biol* **15,** 4791-4802 (1995).
63. Cavadini G et al. TNF-alpha suppresses the expression of clock genes by interfering with E-box-mediated transcription. *Proc Natl Acad Sci U S A* **104,** 12843-12848 (2007).
64. Fukuya H et al. Circadian expression of clock genes in human peripheral leukocytes. *Biochem Biophys Res Commun* **354,** 924-928 (2007).
65. Cockayne DA et al. Urinary bladder hyporeflexia and reduced pain-related behaviour in P2X3-deficient mice. *Nature* **407,** 1011-1015 (2000).